Chapter 5

Isolation, characterization, *in vitro*, and *in vivo* investigation of dihydroartemisinin-loaded bovine milk exosomes

5 Isolation, characterization, *in vitro* and *in vivo* investigation of dihydroartemisinin-loaded bovine milk exosomes

5.1 Background

The study aimed to enhance the efficacy, anti-metastatic properties, and oral bioavailability of DHA while reducing its toxicity by encapsulating it in bovine milk exosomes for the treatment of melanoma (Figure 5.1). Exosomes were derived from bovine milk, and DHA-loaded exosomes were prepared using the sonication method. The exosomal formulations were optimized through a Quality by Design (QbD) approach.

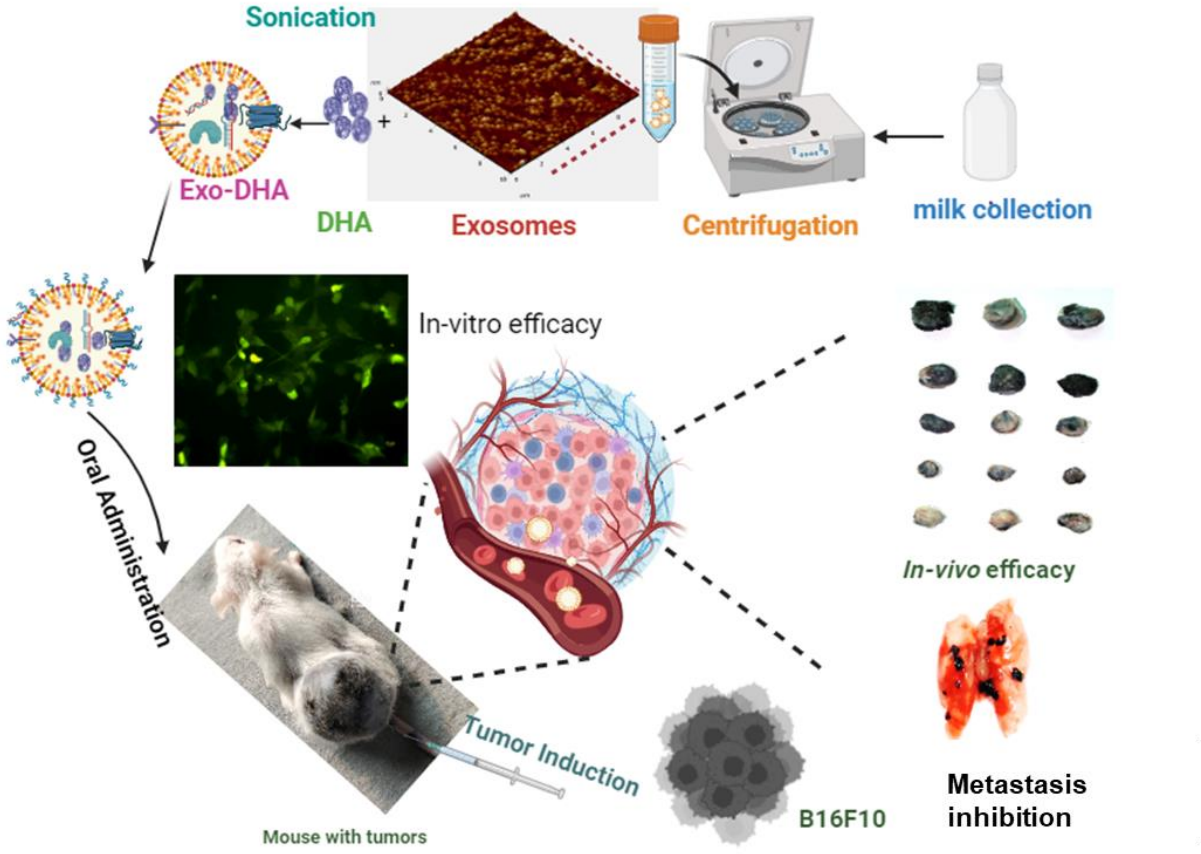

Figure 5.1 Graphical representation of the flow of work for Chapter 5.

Both plain exosomes and DHA-loaded exosomes were characterized based on particle size, morphology, encapsulation efficiency, X-ray diffraction, and drug release behavior at pH 7.4. *In vitro* assessments of Exo-DHA's anti-cancer activity included cytotoxicity, qualitative and quantitative cell uptake assays, reactive oxygen species assays, acridine orange apoptosis

assays, mitochondrial membrane potential assays, and cell migration assays using B16F10 cell lines. Additionally, the impact on oncogene expression was examined via western blotting. *In vivo* efficacy and anti-metastatic effects were evaluated using a B16F10-induced melanoma model, with toxicity profiles assessed through histopathology and biochemical analyses.

5.2 Objectives

- Isolation of exosomes from bovine milk and dihydroartemisinin loading via sonication method and optimization of formulation using Box-Behnken design (BBD) of Design-Expert® software.
- Pharmaceutical characterizations and stability studies of dihydroartemisinin-loaded (Exo-DHA) exosomes
- *In vitro* anti-cancer efficacy and anti-migration studies
- *In vivo* oral bioavailability study
- *In vivo* anti-cancer efficacy study and anti-migration study in melanoma (B16F10) bearing Swiss mice.

5.3 Methodology

5.3.1 HPLC analysis

5.3.1.1 In vitro analytical method

Method development

To determine the concentration of DHA in exosomes, we first developed and validated an HPLC method. The HPLC system used was an Infinity 1200 from Agilent, featuring a quaternary pump, an autosampler unit, and a 1200 photodiode array (PDA) detector, all controlled by Open LAB CDS EZChrom Workstation VL software. The stock solution of DHA (100 µg/ml) was prepared by dissolving 5 mg in 50 ml of HPLC-grade methanol and diluted to appropriate concentrations as working standard solutions. Chromatographic separations were performed using a reversed-phase C18 column (250 mm×4.6 mm, 5 µm; Thermo

Scientific, USA), with the parameters listed in Table 5.1. The calibration curve was generated using a concentration range of 2-20 µg/ml.

Table 5.1 HPLC parameters for DHA method development and validation

Parameters	Values
Mobile Phase	Methanol : water (80:20)
Column	RP- C18 (250 mm×4.6 mm. 5 µm; Thermo Scientific, USA)
Elution	Isocratic
Flow Rate	1 ml/min
Retention Time	3.8 min
Run Time	10 min
Column Temp.	25°C
λ_{max}	266 nm
Injection Volume	10 µl
Detector	PDA
LC Software	Open LAB CDS EZChrom Workstation VL software

Method validation

The developed method was validated in accordance with ICH guidelines, evaluating parameters such as linearity, accuracy, precision, and specificity. The serial dilution technique was utilized to determine the Limit of Detection (LOD) and Limit of Quantification (LOQ) (Guideline, 1997) [173].

Linearity

The linearity of the methods employed for DHA analysis was assessed by constructing a standard curve correlating various analyte concentrations with the corresponding peak areas (detector responses). The concentration range was chosen based on expected drug concentrations in drug loading and drug release studies. Calibration curves consisting of eight points were generated over three consecutive days using standard working solutions. These solutions were injected in triplicate into the HPLC system. The linearity of the analytical methods was evaluated by plotting the peak area (detector response) against the analyte concentration. Linear regression analysis was performed to determine the slope, intercept, and coefficient of correlation (r^2).

Accuracy

Quality control (QC) samples at three distinct concentrations were analyzed to assess the accuracy of the analytical method for DHA. The analysis was performed in triplicate (n = 3). The accuracy of the HPLC method was investigated from the percentage recovery by the standard addition method at three levels (50, 100, and 150%). Accurately 4, 8, and 12 µg/mL of working standard solution were added to pre-analyzed samples (8 µg/mL) to produce 6, 8, and 10 µg/mL, respectively. The samples were analyzed by the developed HPLC method for quantifying the DHA. The percent recovery was calculated by the equation below.

$$\% \text{ recovery} = \frac{Experimental\ or\ recovered\ concentration}{Theoretical\ concentration\ after\ addition} X\ 100$$

Precision

The precision (% RSD) of the method was evaluated by calculating the intra- and inter-day coefficient of variation. Intra-day precision was determined by analyzing three different concentrations of the drug in triplicate, conducted three times on the same day. Inter-day precision was evaluated by performing the same analysis on separate days, with the procedure repeated over three consecutive days.

Sensitivity (Detection and Quantitation limit)

The sensitivity of the analytical method is predicted by the lower limit of detection (LOD) and lower limit of quantitation (LOQ). LOD is the lowest detectable concentration of the analyte while LOQ is the lowest amount of the analyte in a sample, which could be quantitatively determined with suitable precision and accuracy. LOQ was assessed by standard deviation of the response and the slope (S). Standard deviation was estimated by running the five blank samples while the slope was determined based on the calibration curve. LOD and LOQ for DHA were determined following the guidelines of ICH (Guideline, 1997).

Robustness

The robustness of the developed HPLC method was studied by intentional changes in different chromatographic settings, such as wavelength (264, 266, and 268 nm), run times (8, 10, and 12 min), flow rate (0.8, 1, and 1.2 mL/min), mobile phase composition (78:22, 80:20, and 82:18 v/v of methanol:water), and analyzing the changes in the peak area and retention time (Rt) DHA of 12 µg/mL.

5.3.1.2 *In vivo* analytical method

The in vivo analytical method development and validation were carried out on the same HPLC system as employed during the analysis of the in vitro samples. The parameters for method development are given in the table below (Table 5.2).

Table 5.2 HPLC parameters for DHA method development and validation for in vivo analysis

Parameters	Values
Mobile Phase	Methanol : water (80:20)
Column	RP- C18 (250 mm×4.6 mm. 5 µm; Thermo Scientific, USA)
Elution	Isocratic
Flow Rate	1 ml/min
Retention Time	3.8 min
Run Time	10 min
Column Temp.	25°C
λ_{max}	266 nm
Injection Volume	10 µl
Detector	PDA
LC Software	Open LAB CDS EZChrom Workstation VL software

Sample preparation

Blood was collected from the retro-orbital plexus of female rats into the heparinized microcentrifuge tubes. Plasma was separated by centrifuging the blood at 10,000 rpm for 5 min at 4°C. Blank plasma (150 µl) was spiked with different concentrations of working standard solutions (50 µl) to give respective sets of calibration curve standards and QC samples. The plasma (50 µl) was mixed with 50 µl different concentrations of the DHA (0.05 µg/ml to 25.6 µg/ml). A protein precipitating agent ACN (500 µl) was added and vortexed for 10 min. The mixture was centrifuged at 12,000 rpm for 10 min. After centrifugation supernatant was dried in a vacuum drier at 40°C. The dried sample was reconstituted by adding 60 µl of mobile phase

and transferred to auto-sampler vials, capped, and placed in the HPLC autosampler. A 50 µl aliquot of each sample was injected into the HPLC column (system specifications are similar to the in vitro method).

Linearity and range

The linearity of the developed HPLC method was identified by observing the correlation coefficients obtained from the calibration curves of DHA. The range of linearity was determined by fitting the data of average area (mAU) of three independent analyses with the corresponding concentration (μ g/mL) to the linear equation and determining the concentrations range that follows the linearity.

Accuracy

Quality control (QC) samples at three distinct concentrations were analyzed to assess the accuracy of the analytical method for DHA. The analysis was performed in triplicate (n = 3). The accuracy of the HPLC method was investigated from the percentage recovery by the standard addition method at three levels (50, 100, and 150%). Accurately 4, 8, and 12 µg/mL of working standard solution were added to pre-analyzed samples (8 µg/mL) to produce 6, 8, and 10 µg/mL, respectively. The samples were analyzed by the developed HPLC method for quantifying the DHA. The percent recovery was calculated by the equation below.

$$\% \text{ recovery} = \frac{Experimental\ or\ recovered\ concentration}{Theoretical\ concentration\ after\ addition} X\ 100$$

Precision

The precision (% RSD) of the method was evaluated by calculating the intra- and inter-day coefficient of variation. Intra-day precision was determined by analyzing three different concentrations of the drug in triplicate, conducted three times on the same day. Inter-day precision was evaluated by performing the same analysis on separate days, with the procedure repeated over three consecutive days.

Sensitivity (Detection and Quantitation limit)

The sensitivity of the analytical method is predicted by the lower limit of detection (LOD) and lower limit of quantitation (LOQ). LOD is the lowest detectable concentration of the analyte while LOQ is the lowest amount of the analyte in a sample, which could be quantitatively determined with suitable precision and accuracy. LOQ was assessed by standard deviation of the response and the slope (S). Standard deviation was estimated by running the five blank samples while the slope was determined based on the calibration curve. LOD and LOQ for DHA were determined following the guidelines of ICH (Guideline, 1997).

Robustness

The robustness of the developed HPLC method was studied by intentional changes in different chromatographic settings, such as wavelength (264, 266, and 268 nm), run times (8, 10, and 12 min), flow rate (0.8, 1, and 1.2 mL/min), mobile phase composition (78:22, 80:20, and 82:18 v/v of methanol:water), and analyzing the changes in the peak area and retention time (Rt) DHA of 12 µg/mL.

5.3.2 Isolation of exosomes

Exosomes (Exo) were isolated from raw bovine milk, as obtained from the dairy farm located in the BHU campus, Varanasi, India, followed by multiple centrifugation processes as discussed by Munagal et al. 2016 [174]. Raw bovine milk was first centrifuged at 13,000 rcf for 30 minutes at 4ºC to remove fat.

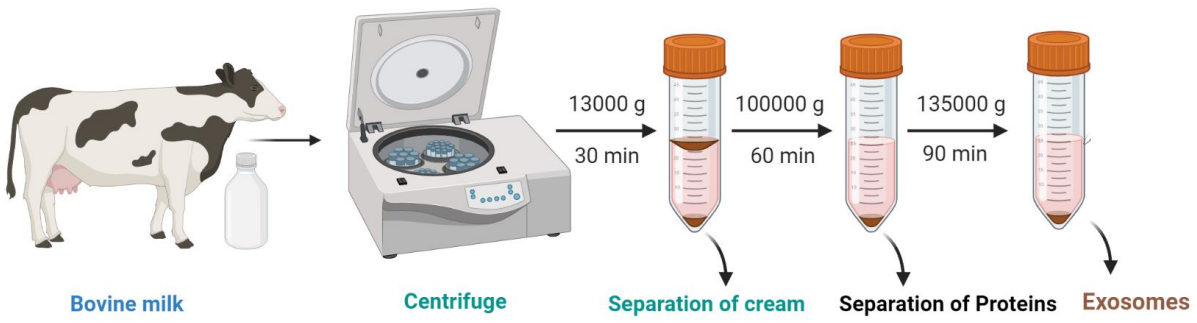

Figure 5.2 Schematic diagram of isolation of exosomes from bovine milk.

The supernatant was then ultracentrifuged at 100,000 rcf for 60 minutes at 4ºC to eliminate microvesicles. After collecting the supernatant, it underwent a second ultracentrifugation at 130,000 rcf for 90 minutes. The resulting pellets were washed twice with cold PBS and redispersed using a manual homogenizer. The exosome solution was then filtered through 0.22µm PVDF syringe filters, and the protein content was measured using the Bradford assay before storing at -80ºC.

5.3.3 Immunoblotting analysis

Immunoblotting was performed to confirm the purity of isolated exosomes. The detection of exosomal surface biomarkers such as CD63, CD81, Tsg101, and Alix using antibodies from Cell Signaling (Danvers, MA) confirmed the exosomes. On the other hand, markers for multivesicular bodies (MVBs) like β1 integrin, p-selectin, and CD40 were examined to rule out MVBs contamination and confirm the purity of exosomes. Secondary antibodies suitable for the experiment were utilized, and protein detection was achieved using Enhanced Chemiluminescence (ECL) Prime western blotting detection reagent from Cytiva (Amersham). The loading control for protein was verified using β-actin antibodies from Sigma-Aldrich (St. Louis, MO).

5.3.4 Preparation of drug-loaded exosomes

Table 5.3 Different levels and constraints for variables in BBD

Independent Variables	**Levels**		
	-1	**0**	**+1**
A; Amount of exosomes (mg)	1	5	9
B; Amount of drug (mg)	1	5	9
C; Sonication time (sec)	60	120	180
Dependent Variables	**Constraints**		
Particle size (nm)	< 200		
PDI	<0.3		
%EE	Maximum		
%DL	Maximum		

Table 5.4 The runs obtained from the Box Behnken Design

Run	Factor 1 A: Amount of Exo (mg)	Factor 2 B: Amount of drug (mg)	Factor 3 C: Sonication time (sec)
1	1	10	120
2	5.5	10	60
3	10	10	120
4	5.5	5.5	120
5	5.5	5.5	120
6	10	1	120
7	5.5	5.5	120
8	5.5	10	180
9	5.5	1	60
10	5.5	5.5	120
11	1	1	120
12	10	5.5	180
13	5.5	5.5	120
14	5.5	1	180
15	10	5.5	60
16	1	5.5	60
17	1	5.5	180

To prepare the DHA-loaded exosomes with desired quality attributes *viz.* smaller particle size, narrow size distribution, maximum encapsulation efficiency, drug loading, etc., the Quality by Design (QbD) approach was employed. This approach establishes an interaction between critical quality attributes (CQAs), critical material attributes (CMAs), and critical process parameters (CPP). Also, applying QbD reduces the experimental runs required to fabricate optimized DHA-loaded exosomes. In the present study, Box Behnken Design (BBD) was employed using 3-factors and 3 levels (Design-Expert 12, State-Ease Inc, Minneapolis, USA) [175, 176]. Table 5.3 summarizes the independent variables (factors), their levels, and the constraints of the dependent variables (response) in BBD. Table 5.4 shows the different experimental runs obtained from the BBD.

DHA-loaded exosomes (Exo-DHA) were prepared using the sonication method [177]. DHA was dissolved in a 1:1 ethanol-acetonitrile mixture and combined with the exosomal solution at different ratios (Table 5.4). The mixture was sonicated at 20% amplitude for six cycles (30

seconds on/off, with a 2-minute gap between cycles). After sonication, Exo-DHA was kept at room temperature for 1 hour to allow the exosomal membrane to recover. Exo-DHA was then centrifuged at 10,000 x g for 10 minutes to remove any precipitation and unbound drug, followed by ultracentrifugation at 130,000 x g for 90 minutes. The resulting pellets were washed twice with chilled PBS and stored at -80ºC until use.

5.3.5 Drug loading analysis

To determine the percent drug loading (%DL) and percent encapsulation efficiency (%EE), Exo-DHA (0.3 ml) was mixed with methanol (0.7 ml) followed by vortexing to extract the drug from the exosomes. The mixture was centrifuged at 10,000 x g for 10 min to precipitate the protein. The supernatant was collected and used for determining the drug concentration by using the HPLC method using the following formula [178];

$$\textbf{Encapsulation efficiency (\%)} = \frac{\textit{Amount of drug encapsulated in exosomes}}{\textit{Total amount of drug added}} \textbf{X100}$$

$$\textbf{Drug loading (\%)} = \frac{\textit{Amount of drug encapsulated in exosomes}}{\textit{Total amount of drug and Exosomes in final formulation}} \textbf{X100}$$

5.3.6 Characterization

The developed DHA-loaded exosomes (Exo-DHA) were characterized for average particle size, polydispersity index (PDI), and zeta potential (ZP) using DelsaNano particle analyzer (DelsaNano, Beckman coulter, CA, USA). The morphology of Exo and Exo-DHA was observed through scanning electron microscopy (SEM) (Nova Nao SEM 450, FEI, Hillsboro, OR, USA) and atomic force microscopy (AFM) (INTEGRA Prima, NT-MDT Service & Logistics Ltd, Tempe, AZ, USA). For the SEM analysis, 20 µl of Exo and Exo-DHA was diluted 500 times with fresh PBS and filtered through 0.22 µm PVDF syringe filters. Each sample (10 µl) was placed in glass slides and air-dried, followed by coating with gold, and observed under the scanning electron microscope [179]. The sample preparation for the AFM was the same as that of SEM, where 10 µl of the sample was placed on clean glass slides and

allowed to dry at room temperature. Images were obtained by displaying the amplitude signal of the cantilever in the trace direction, and the height signal in the retrace direction, both signals being simultaneously recorded.

5.3.7 X-Ray diffraction

The X-Ray diffraction (XRD) pattern of Exo, DHA, and Exo-DHA was examined using HR-XRD operating at 9kW power and a diffraction angle ranging from 10 to 40º with a 10º/min scan rate. The liquid samples were dropped multiple times on small glass slides until a thin film was formed, followed by placing the slide on a goniometer and recording the diffraction pattern using the DTEX detector [180].

5.3.8 Stability study

The stability of Exo and Exo-DHA was analyzed by determining size, PDI, and zeta potential for one month at -80ºC. The samples were withdrawn weekly for one month and analyzed for the above-mentioned parameters.

5.3.9 Drug release

The *in vitro* drug release study was performed to determine the rate and extent of drug release at pH 7.4 and pH 5.5, as described previously [181, 182]. Before starting the experiment, the dialysis bags (MWCO 14000 Da, Himedia, Mumbai, India) were soaked in PBS overnight for activation. After that, 1 mg of each DHA and Exo-DHA was loaded into dialysis bags and suspended in 50 ml of corresponding medium containing 0.2% of tween 80 to maintain the sink conditions and placed on a multiple-mode magnetic stirrer (37ºC, 200 rpm). Sample (3 ml) was withdrawn at 0, 0.5, 1, 2, 4, 6, 8, 10, 12, 24, and 48 h and replaced with the same volume of fresh PBS. The drug concentrations were then analyzed using HPLC (Infinity 1200, Agilent Technologies, CA, USA).

5.3.10 Cell culture and conditions

B16F10 cell lines were purchased from the National Center for Cell Science (NCCS), Pune, Maharashtra, India. Cell lines were cultured in DMEM medium, supplemented with 10% fetal

bovine serum (Gibco, Thermo Fisher), 1% Anti-biotic and anti-mitotic solution (Himedia, Mumbai, India) (10,000 U Penicillin, 10 mg streptomycin, 25 µg Amphotericin B per ml) and grown at 37°C temperature in a humidified incubator (Heracell VIOS 160i, Thermo fisher. MA, USA).

5.3.11 Cytotoxicity study

The cytotoxic effect of Exo, DHA, and Exo-DHA in B16F10 and HEK-293 cells was measured by MTT assay as described in previous reports [183]. Briefly, B16F10 cells were seeded in 96 well plates at 1 x 10^4 cells/well density and incubated overnight at 37ºC. After 24 h, the media was aspirated, and fresh media was added containing Exo, DHA, and Exo-DHA at different concentrations and incubated for 24, 48, and 72 h. At the end of each treatment period, the media was removed, and cells were washed with chilled PBS. Then, 100 µl of MTT dye (0.5 mg/ml) was added to each well and incubated for 4 h. After that, the MTT solution was aspirated carefully, and insoluble formazan crystals were dissolved by adding the same amount of cell culture-grade DMSO and incubated for 30 min. The optical density was measured using a spectrofluorometer (BioTek) at a lambda max of 570 nm. The percent of cell viability was estimated, and IC50 was calculated with GraphPad Prism software.

5.3.12 Qualitative cell uptake assay

To check the uptake capability and internalization of drug-loaded exosomes into the cancer cells, a qualitative cell uptake assay was performed with coumarin-6 (C-6) loaded exosomes, as discussed in [184]. C-6 was loaded into exosomes following the same procedure as the drug loading method, with C-6 replacing the drug. Cells were seeded in 35 mm tissue culture dishes (Abdos, Roorkee, India) at the density of 5 x 10^5 cells in each dish and incubated overnight. After that, the cells were washed and incubated with C-6-loaded exosomes (3 µg/ml) for 4 h, washed with cold PBS, and observed under a fluorescence microscope (Olympus BX53, Tokyo, Japan).

5.3.13 Apoptosis assay by 4,6-Diamidino-2-phenylindole (DAPI) staining

The qualitative cell apoptosis assay via DNA fragmentation (DAPI staining) was performed as described in [185]. Briefly, B16F10 cells were seeded on 8 well-chambered tissue slides (SPL life sciences Co Ltd, Naechon-Myeon, South Korea) at the density of 5 x 10^4 cells/well and incubated overnight for cell attachment followed by treatment with Exo (10 µg/ml), DHA, and Exo-DHA (equivalent to 36 µM of DHA) and further incubated for 24 h. After completion of the incubation period, the media was aspirated, and cells were washed with chilled PBS to remove any drug content, followed by incubation with fresh media containing DAPI (5 µg/ml) for 10 minutes. After incubation, media was removed, and cells were washed with fresh, chilled PBS and observed under a fluorescence microscope (Olympus BX53, Tokyo, Japan) [186].

5.3.14 Apoptosis assay

The qualitative cell apoptosis assay was performed by using an ethidium bromide/Acridine orange (4',6-diamidino-2-phenylindole) staining kit (Thermo Scientific, MA, USA) [186]. B16F10 cells were seeded in 8 well-chambered slides (SPL life sciences) at a density of 5 x 10^5 cells/well and incubated in a CO2 incubator overnight. Subsequently, the media was aspirated, and fresh media was provided containing different exosomal DHA formulations (equivalent to 36 µM of DHA) followed by incubation for 24 h. After the completion of the treatment period, cells were washed with cold PBS and further incubated with 15 µl of ethidium bromide/ Acridine orange (4',6-diamidino-2-phenylindole) staining kit as per manufacturer protocol for 20 minutes. The cells were then washed with PBS again and examined under a fluorescence microscope (Olympus BX53, Tokyo, Japan).

5.3.15 Reactive oxygen species assay

H_2DCFDA dye was used to assess the production of intracellular oxygen species as described previously [187]. For the attachment, the cells were seeded in 35 mm sterile cell culture petri dishes at a density of 5 x 10^5 cells/well and incubated overnight at 37°C. After 24 h, the media

was removed, and fresh media containing Exo (10 µg/ml), DHA, and Exo-DHA (equivalent to 36 µM of DHA) was added and incubated for 24 h. Cells were given 0.05% H_2O_2 treatment as a positive control two hours before the end of the treatment period. In the following treatment, 10 µM of H2DCFDA was added to each petri dish and incubated further 30 min, followed by washing with chilled PBS, and fluorescence was observed under the fluorescence microscope (Olympus BX53, Tokyo, Japan). For the flow cytometry analysis, after the treatment period, cells were collected by trypsinization followed by treatment with 500 µl of 10 µM of H_2DCFDA and incubated for 30 minutes. After that, ROS generation was analyzed with a flow cytometer (CytoFlex LX, Beckman coulter, MA, USA).

5.3.16 Mitochondrial membrane potential assay

DHA inhibits cancer cell growth via different mechanisms of action, and inhibition of mitochondrial membrane potential (MMP) is one of them [188]. MMP assay was performed to investigate the capability of DHA and Exo-DHA in inhibiting MMP in B16F10 cell lines. Briefly, B16F10 cells at the density of 5 x 10^5 were seeded in 8 well-chambered tissue culture slides (SPL life sciences Co Ltd, Naechon-Myeon, South Korea) and incubated in a humidified chamber overnight. After the incubation period, cells were washed, and treatment was provided with different formulations (Exo (10 µg/ml), DHA, Exo-DHA; equivalent to 36 µM of DHA) for 24 h. After the completion of the treatment period, the media was removed, and fresh media was added containing JC-1 dye (10 µg/ml) and incubated for 30 minutes. Following the incubation, the dye was removed, washed with fresh, chilled PBS, and observed in a fluorescence microscope (Olympus BX53, Tokyo, Japan).

5.3.17 Colony formation assay

A colony formation assay is an *in vitro* cell survival assay based on the capability of growing a single cell into the colony, and it was performed as described previously (Figure 5.3) [189]. Briefly, 100 cells were seeded individually in each 60 mm petri dish and incubated overnight

at 37ºC. Media was aspirated after the incubation period, and fresh media was added containing Exo (10 µg/ml), DHA, and Exo-DHA (equivalent to 36 µM of DHA) and incubated for a further 24 h. After that, the media was removed, and fresh media was added every alternative day for ten days, followed by staining with 0.5% crystal violet. The number of colonies was counted manually.

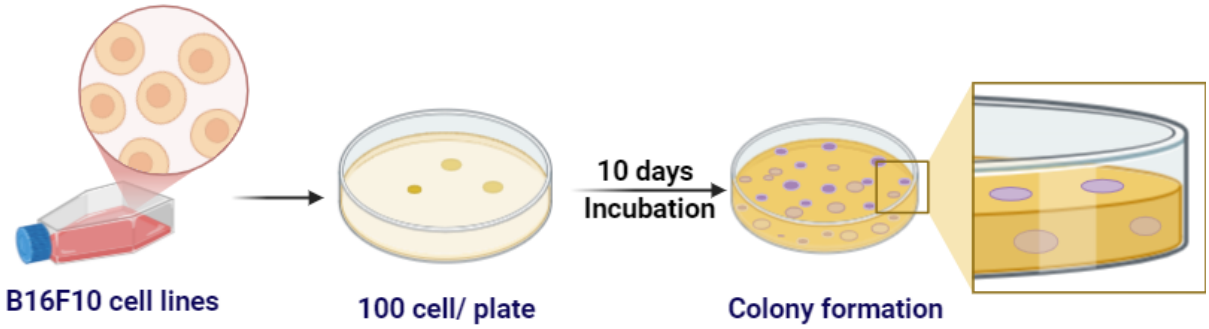

Figure 5.3 Graphical representation of the procedure for colony formation assay.

5.3.18 Cell migration assay

The cell migration assay was performed to check the migration inhibition property of developed exosomal formulations in 6 transwell chambers (Sigma Aldrich, MA, USA) (Figure 5.4). Briefly, B16F10 cells were pretreated with the Exo (10 µg/ml), DHA, and Exo-DHA (equivalent to 20 µM of DHA) for 1 h then cells were harvested via the trypsinization process; after that, 0.5 ml of cells were seeded in 6 transwell upper chambers without FBS (only media) at the density of 4×10^2 cells/100 µL and media containing 10% FBS were added to the lower chamber which acted as chemoattractant and incubated for 24 h. After incubation, the migrated cells were fixed with the 4% formaldehyde, and stained with 0.5% toluidine blue. The number of migrated cells was counted on an inverted microscope (Dewinter, New Delhi, India).

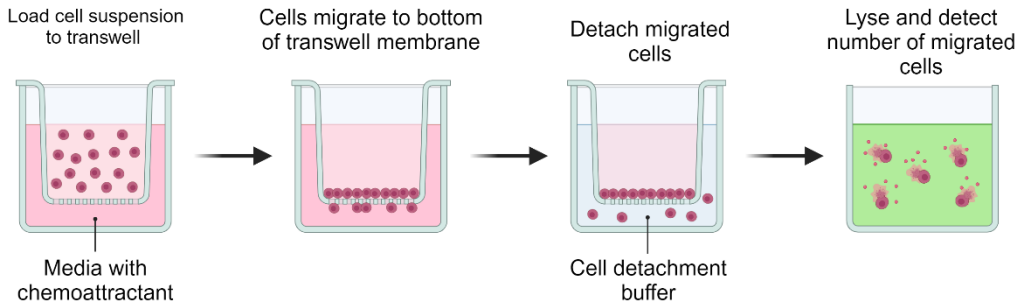

Figure 5.4 Graphical representation of *in vitro* transwell migration assay.

5.3.19 Wound healing assay

The wound healing assay for Exo, DHA, and Exo-DHA was conducted as shown in Figure 5.5 [190]. Briefly, 200 µl of B16F10 cells were seeded into Culture-insert 2 wells (Ibidi, Germany) at a density of 1 x 10^5 cells/100 µl and incubated for 12 h. After cell attachment, the culture inserts were carefully removed with sterile forceps to create the wound. The cells were then washed with chilled PBS, treated with Exo (10 µg/ml), DHA, and Exo-DHA (equivalent to 36 µM DHA), and incubated for 24 h. Wound healing was observed under an inverted microscope at 0, 12, and 24 h. The percentage of wound healing was calculated using Image J software. The rate of wound closure was calculated by using the following formula;

$$\text{Rate of wound closure} = \frac{Distance\ wound\ closing\ (\mu m)}{Time\ (hours)}$$

Distance wound closing= Initial wound distance-final wound distance

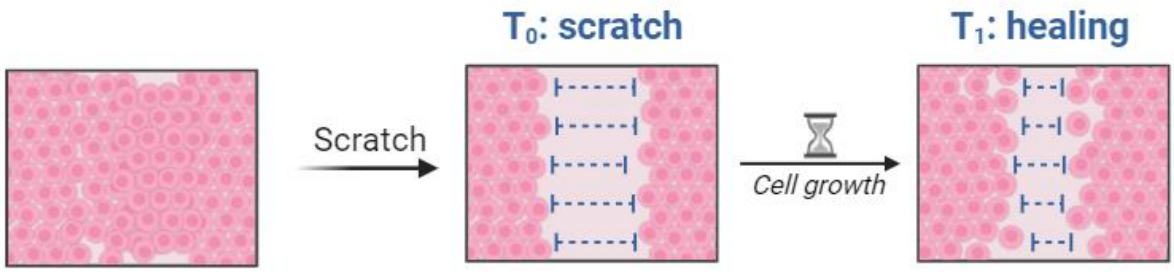

Figure 5.5 Graphical representation of wound healing assay.

5.3.20 Immunoblotting

To investigate the efficacy of DHA and Exo-DHA on the expression of apoptotic, anti-apoptotic, and proteins involved in metastasis, western blotting was performed as discussed in [191]. Briefly, B16F10 cells were seeded in 6 well plates (Tarson, India) at the density of 1 x 10^6 cells/well and incubated overnight, followed by treatment with different formulations and further incubated for 24 h (equivalent to 36 µM of DHA). After the completion of the treatment period, the cells were scrapped with a sterile cell scraper. Cell pellets were collected by centrifugation, suspended in RIPA buffer, and incubated for 1 hour on ice with intermediate stirring. Following that, the lysed cells were centrifuged at 15,000 rpm for 30 minutes at 4ºC, and the supernatant was estimated for protein concentration via Bradford assay. An equal amount of protein samples (30 µg) were loaded on SDS-PAGE (8-15%) and after the completion of the electrophoresis process, the protein bands were transferred onto the PVDF membrane. The PVDF membrane was blocked with 5% milk for 2 h, followed by incubation with primary antibodies of Bcl-2, Bax, Survivin, and MMP-9 at 4ºC overnight. After the overnight incubation, the membrane was washed with tris-buffered saline and 0.01% tween 20, followed by incubation with respected secondary antibodies for 2 h. Finally, the chemiluminescence signals were detected using Immobilon Western chemiluminescent (Millipore) with Chemi Doc system (BioRad, CA, USA), and images were quantified using Image J software (NIH, Bethesda, USA).

5.3.21 Animal studies

All the animal studies were approved by the Institutional Animal Ethics Committee, Department of Pharmaceutical Engineering and Technology, IIT (BHU), approval no IIT(BHU)/IAEC/2023/002 and CPCSEA guidelines were followed for the housing of animals. The animals (for pharmacokinetics and tissue biodistribution studies, female Sprague Dawley rats 10-12 weeks old, and for *in vivo* efficacy and metastasis studies, female Swiss albino mice

8-10 weeks old) were purchased from the Institute of Medical Science Animal House, Banaras Hindu University (BHU), Varanasi, India and maintained in the 12 hours dark 12 hours day and provided water food ad libitum.

5.3.22 Pharmacokinetics

The female Sprague Dawley rats (aged 10-12 weeks) were divided into two groups, each consisting of 5 rats (n=5/group): Group I received DHA, and Group II received Exo-DHA. Before the start of the experiment, the animals underwent a 12-hour fasting period. Subsequently, a single dose of DHA (suspended in 0.5% carboxymethyl cellulose, 50 mg/kg) and Exo-DHA (Equivalent to 50 mg/kg of DHA) was administered orally. Following the administration of the single dose, blood samples (200 µl) were collected from the retro-orbital vein of the rats at predetermined time intervals (0.25, 0.5, 1, 2, 4, 6, 8, 10, 12, and 24 hours) under mild anesthesia and placed in heparinized centrifuge tubes. The collected blood was then centrifuged at 10000 rpm for 10 minutes at 4ºC to obtain plasma. The plasma, containing the drug, was extracted using methanol and filtered through 0.22 µm nylon membrane filters (Merck, Bangalore, India) for analysis. The samples were analyzed via HPLC instrument (Infinity 1200, Agilent, USA) as per the validated method. The pharmacokinetic parameters, such as AUC, Tmax, Cmax, elimination half-life, etc. were calculated via PK solver software.

5.3.23 Tissue distribution

For the *in vivo* tissue distribution study, female Sprague Dawley rats were divided into two groups, with each group containing 5 rats (n=5/group): Group I received DHA, and Group II received Exo-DHA. A single oral dose, equivalent to 50 mg/kg of DHA, was administered to both groups. After 8 hours post-dosing, the animals were humanely sacrificed via cervical dislocation. Vital organs such as the intestine, lungs, liver, heart, kidney, and spleen were carefully collected and washed with chilled PBS to remove any external contaminants. Subsequently, all the organs were weighed, and homogenized using a tissue manual

homogenizer to ensure uniformity. The drug was extracted from the homogenized tissue samples by adding methanol, followed by centrifugation at 15000 rpm for 20 minutes. The resulting supernatant containing the drug was collected and filtered using 0.22 µm nylon filters to remove any particulate matter. The concentration of the drug in each organ was then estimated using HPLC, allowing for the determination of the tissue distribution of DHA in the various organs of interest following different treatments.

5.3.24 *In vivo* anti-cancer efficacy study

The *in vivo* anti-cancer efficacy of different formulations and free drugs was investigated in 8-week-old Swiss albino mice (Figure 5.6). Before the experiment, the animals underwent a 7-day acclimatization period with access to water and food ad libitum. B16F10 cells were cultured in the 10% FBS-added DMEM media. After reaching 90% confluency, cells were harvested by trypsin and then adjusted to 5 x 10^5 cells/100µl of cell culture media and inoculated into the dorsal side of each mouse subcutaneously

Figure 5.6 Graphical representation of tumor model development and treatments in Swiss mice . Tumor size was measured every alternative day. After reaching the size of the tumor to 60-80 mm^3 the animals were separated into different groups Group I: Control (no treatment), Group II: Exosomes (25 mg/kg, Orally), Group III: DHA (50 mg/kg, Orally), Group IV: Exo-DHA (equivalent to 50 mg/kg of DHA, Orally), and Group V: Dacarbazine (DTIC) at 5 mg/kg via intraperitoneal. Additionally, healthy animals were included for toxicity comparison.

Treatments were given three times a week for 20 days (every alternative day), and tumor volume and body weights were measured every alternative day till the end of the experiment. After completing the treatment period, blood was collected from the retro-orbital vein to assess the biochemical parameters. Then, the animals were humanely sacrificed via cervical dislocation, and vital organs (liver, heart, spleen, lungs, and kidney) and tumors were collected for further studies.

5.3.25 Evaluation of toxicity via biochemical and hematological parameters

After the end of the *in vivo* efficacy study, the biochemical and hematological parameters were evaluated for the toxicity assessment as described previously [192]. Hematological parameters were analyzed by collecting 150 µl of blood from the retro-orbital plexus into heparinized centrifuge tubes before euthanizing the animals. Parameters such as white blood cells, red blood cells, platelets, etc., were quantified using an automated hemato analyzer (Microbion, Life Sciences, New Delhi, India). The serum was separated to analyze various biochemical parameters including ALT, AST, ALP, urea, and creatinine by using kit-based assays (ARKAY healthcare PVT, LTD, Gujarat, India) with a biochemical analyzer (CHEM-5-Plus v2, Erba Mannheim, Germany). These analyses were essential for assessing the treatments' potential toxicity and ensuring the experimental procedures' safety.

5.3.26 Histopathology of organs from tumor-bearing mice

The tumor-bearing mice were euthanized at the end of the experiment, and various vital organs such as the liver, lungs, heart, and spleen were collected. These organs were fixed in a 10% formaldehyde solution and subsequently embedded in white paraffin wax blocks. Using a microtome (Leica, Germany), small sections of the blocks (4-5 µm thickness) were cut, and these sections were then stained with hematoxylin and eosin (H&E) to visualize any histopathological changes resulting from the treatments administered. The stained slides were

examined under a microscope (Dewinter, New Delhi, India), and images were captured to document any observed histological alterations.

5.3.27 *In vivo* pulmonary metastasis study

An *in vivo* pulmonary metastasis study was conducted to assess the impact of DHA and Exo-DHA on melanoma metastasis (Figure 5.7). B16F10 melanoma cells were harvested at 90% confluence and injected into the tail vein of mice (5 x 10^5 cells/mouse in 0.2 ml). Mice were randomly divided into four groups (n=5 per group): Group I (control) received PBS, Group II received oral exosomes (25 mg/kg), Group III received oral DHA (50 mg/kg), and Group IV received oral Exo-DHA (equivalent to 50 mg/kg DHA). Treatment began the day after cell injection and continued daily for 20 days. Afterward, the mice were euthanized, and their lungs were collected, washed with chilled PBS, and examined for the number of lung nodules by direct observation, providing data on treatment efficacy in reducing pulmonary metastasis.

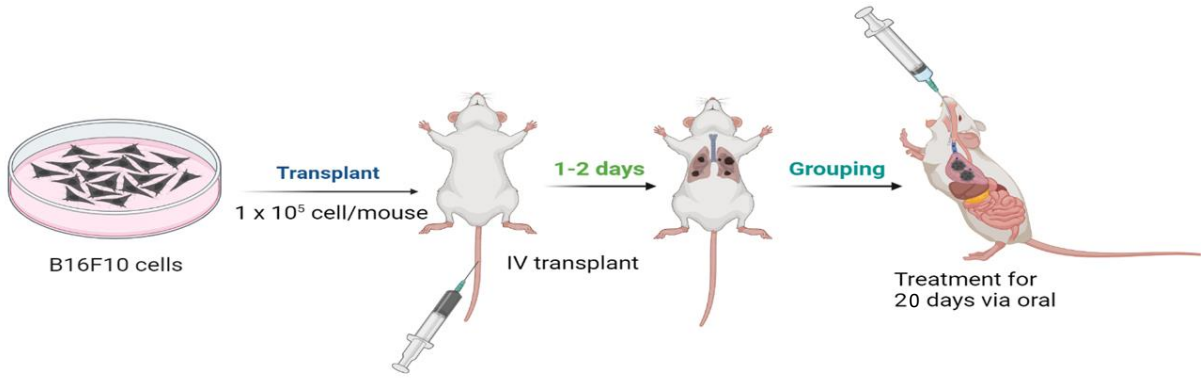

Figure 5.7 Graphical representation for the model development of pulmonary metastasis and treatment in Swiss mice.

5.3.28 Statistical analysis

The results are expressed as mean±SD. The statistical analysis was performed by using One-Way ANOVA followed by a tukey T-test using Graph Pad Prism Version 8.0. The differences were considered significant at a p-value of <0.05 unless stated differently.

5.4 Results and discussion

5.4.1 HPLC Analysis

5.4.1.1 In vitro analytical method

The in vitro analytical HPLC method was developed for DHA to calculate the DHA concentration in the test samples while performing studies like drug loading, encapsulation efficiency determination, and *in vitro* drug release (Figure 5.8).

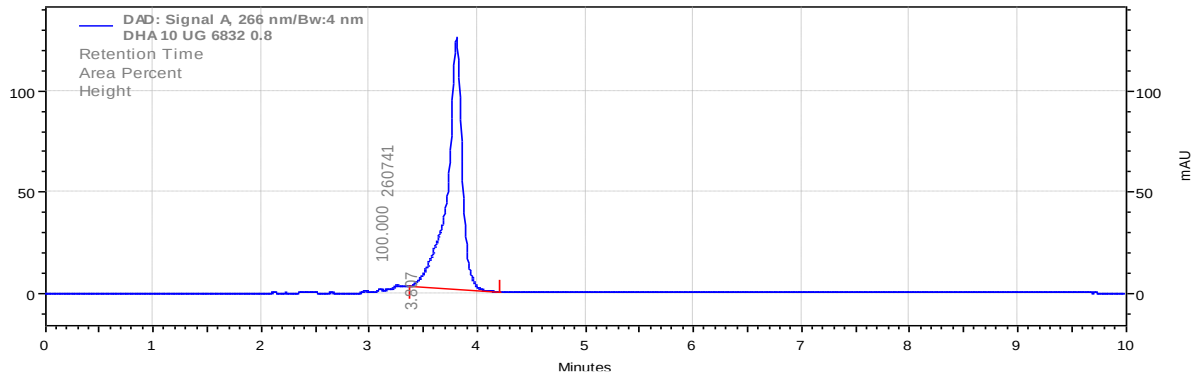

Figure 5.8 The HPLC and DAD signal chromatograms of DHA at wavelength 266 nm, mobile phase methanol: water (80:20).

Linearity and average

Figure 5.9 shows the average area of the triplicate measurements for DHA plotted against the corresponding concentrations. The selected DHA concentrations range from 2 µg/mL to 20 µg/mL, and the Lamda max area (at 266 nm) was shown to be linearly related, with correlation coefficients (r2 = 0.9972) regression equation y = 64256x - 14062.

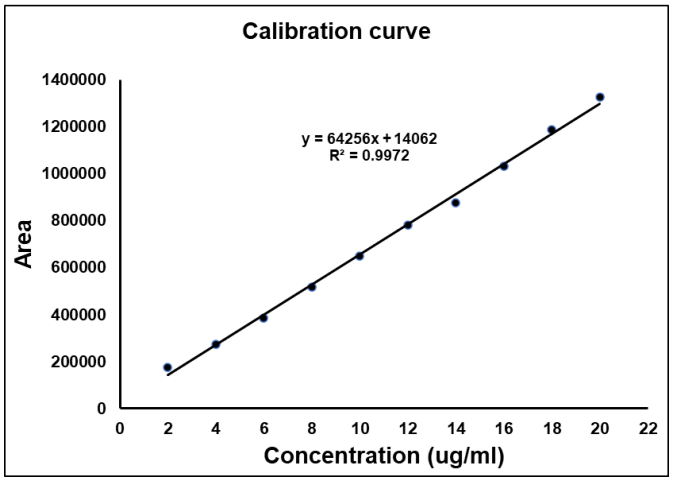

Concentration (µg/ml)	Average peak area
2	175477.7
4	274049.3
6	384243.7
8	517118.7
10	650781.8
12	783128.7
14	877320.7
16	1033775
18	1187060
20	1325771

Figure 5.9 HPLC-based calibration curve of DHA measured at 266 nm.

Accuracy

The accuracy of an analytical method can be assessed by closely comparing its theoretical and experimental values. Table 5.5 presents the DHA accuracy results as the percentage of recovery and the percentage of relative standard deviation (% RSD). The enhanced HPLC method demonstrates exceptional accuracy, as indicated by its high recovery values and low % RSD (<2%).

Table 5.5 Accuracy studies of the developed HPLC method for DHA (n=3)

Concentration of DHA (µg/ml)	Level (%)	DHA Spiked concentration (µg/ml)	Theoretical concentration (µg/ml)	Experimental concentration (µg/ml)	% Recovery	% RSD
8	50	4	6	5.981±0.042	99.68	0.702
8	100	8	8	7.970±0.064	99.62	0.803
8	150	12	10	10.086±0.101	100.86	1.001

Precision

Repeatability and intermediate precision (intra-day and inter-day) experiments were conducted to assess the precision of the HPLC method at various concentrations of the working standard solution (6, 10, and 14 µg/mL). The percentage RSD value from the repeatability analysis was determined to be 1.374% (Table 5.6).

Table 5.7 summarizes the results of the intermediate precision studies. The percentage RSD values for the DHA peak area in intra-day precision studies ranged from 0.54 to 1.03%, while the inter-day precision studies showed percentage RSD values ranging from 0.57 to 0.95%.

Table 5.6 Repeatability study of HES-developed HPLC method (n=8)

Concentration of DHA (µg/ml)	Mean peak area	SD	RSD (%)
10	1105392.4	15195.1	1.374

Table 5.7 Intermediate precision (Intra-day and inter-day precision) studies of the DHA-developed HPLC method

Concentration of DHA (µg/ml)	Intra-day (at an interval of 6 h)	RSD (%)	Inter (Day 1- Day 3)	RSD (%)
	Obtained Avg. peak area±SD (mAU)		Obtained Avg. peak area±SD (mAU)	
2	110876.25±828.58	0.74	109985.56±958.35	0.87
8	795625.05±8208.44	1.03	801065.35±7685.12	0.95
16	1987515.30±10869.40	0.54	1986213.33±11512.31	0.57

LOD and LOQ

The LOD and LOQ values for DHA determination were found to be 0.142 µg/mL and 0.989 µg/mL, respectively. The low LOD and LOQ values demonstrate the HPLC method's high sensitivity for DHA analysis.

Robustness

The robustness measures the HPLC technique's ability to withstand small but deliberate changes in method variables, indicating its reliability under typical operating conditions. The robustness and ruggedness of the established HPLC method were evaluated through intentional modifications across various chromatographic settings. The results showed reduced percentage RSD values (<2%) for both area and retention time (Table 5.8), confirming the method's robustness.

Table 5.8 Robustness and ruggedness study of developed HPLC method for DHA (10 µg/ml)

Parameters	Variations made	Area±SD (mAU)	RSD (%)	Retention time (RT)±SD (min)	RSD (%)
Wavelength	264	102573.23±1491.38	1.45	3.69±0.05	1.35
	266	101741.67±1176.38	1.15	3.89±0.04	1.02
	268	109525.84±848.13	0.77	3.85±0.06	1.55
Run time (min)	8	119256.66±1090.44	1.06	3.78±0.03	0.79
	10	102654.54±1153.33	1.12	3.83±0.06	1.56
	12	121573.51±1014.81	0.83	3.79±0.05	1.31
Flow rate (mL/min)	0.8	118182.65±1248.75	0.96	3.90±0.07	1.28
	1	109021.24±1362.05	1.24	3.88±0.05	1.28
	1.2	100190.89±962.65	0.96	3.57±0.04	1.12
Mobile phase composition (Methanol: Water)	78:22	113237.66±815.68	0.75	3.32±0.03	0.90
	80:20	108018.28±705.52	0.65	3.82±0.03	0.78
	82:18	100149.95±1046.31	1.04	3.95±0.02	0.50

5.4.1.2 *In vivo* analytical method

The HPLC method for DHA was developed in plasma to calculate the DHA concentration in the test samples while performing pharmacokinetic and drug distribution studies. The DHA retention time was found at 3.8 min (Figure 5.10 A), while no drug peak was observed in blank plasma (Figure 5.10 B)

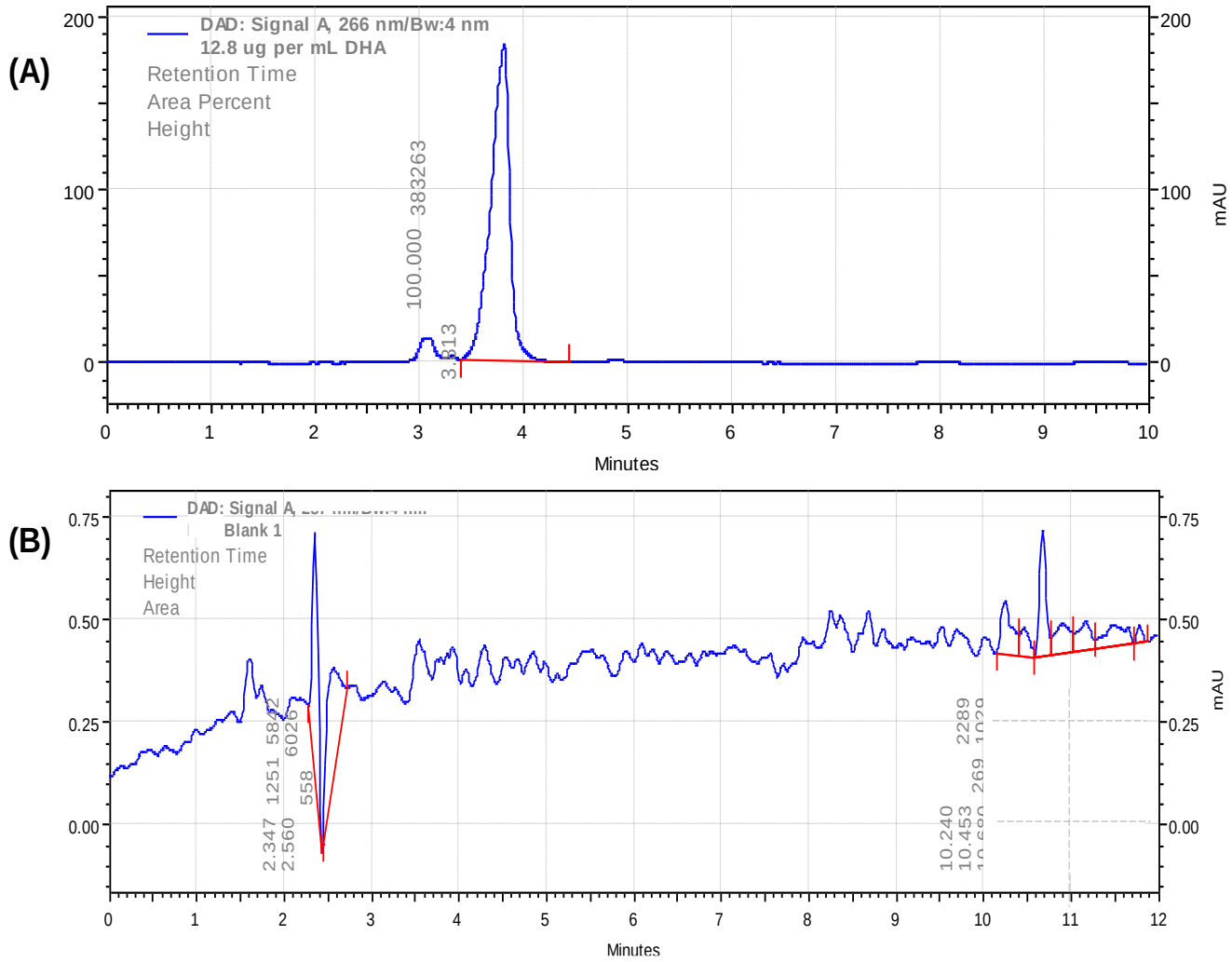

Figure 5.10 (A) HPLC and DAD signal chromatograms of DHA in plasma and (B) blank plasma at wavelength 266 nm, mobile phase methanol: water (80:20).

Linearity and range

Figure 5.11 shows the average area of the triplicate measurements for DHA plotted against the corresponding concentrations.

Concentration	Area
25.6	839667
12.8	384835
6.4	191014
3.2	111011
1.6	53421
0.8	43333
0.4	26251
0.2	16922
0.1	12574
0.05	11152

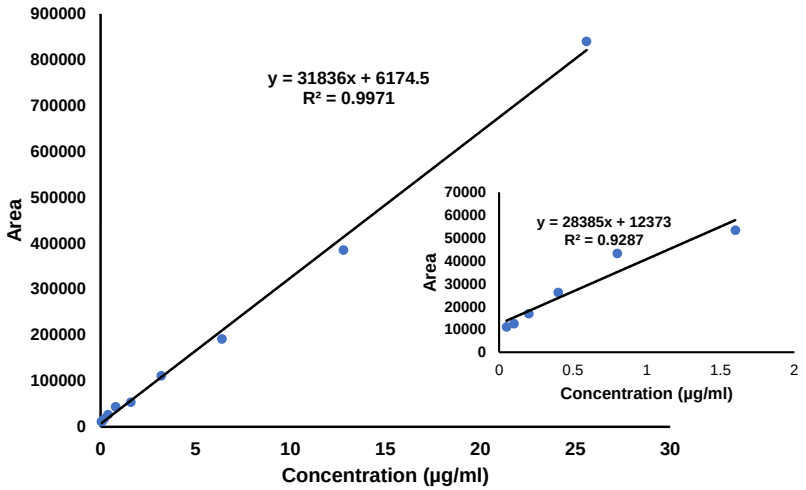

Figure 5.11 HPLC-based calibration curve of DHA in plasma measured at 266 nm.

The selected DHA concentrations range from 0.05 to 25.6 µg/mL, and the Lambda max area (at 266 nm) displayed a linear relationship, with a correlation coefficient of $r^2 = 0.9971$ and a regression equation of y = 31836x - 6174.5.

Accuracy

The accuracy of an analytical method can be assessed by closely comparing its theoretical and experimental values. Table 5.9 presents the DHA accuracy results as the percentage of recovery and the percentage of relative standard deviation (% RSD). The enhanced HPLC method demonstrates exceptional accuracy, as indicated by its high recovery values and low % RSD (<2%).

Table 5.9 Accuracy studies of the developed HPLC method for DHA (n=3)

Concentration of DHA (µg/ml)	Level (%)	DHA Spiked concentration (µg/ml)	Theoretical concentration (µg/ml)	Experimental concentration (µg/ml)	% Recovery	% RSD
8	50	4	6	5.991±0.032	99.48	0.534
8	100	8	8	7.870±0.064	99.56	0.813
8	150	12	10	10.096±0.121	100.96	1.198

Precision

Table 5.10 Repeatability study of HES-developed HPLC method (n=8)

Concentration of DHA (µg/ml)	Mean peak area	SD	RSD (%)
10	1206392.4	16185.1	1.3416

Table 5.11 Intermediate precision (Intra-day and inter-day precision) studies of the DHA-developed HPLC method

Concentration of DHA (µg/ml)	Intra-day (at an interval of 6 h)	RSD (%)	Inter (Day 1- Day 3)	RSD (%)
	Obtained Avg. peak area±SD (mAU)		Obtained Avg. peak area±SD (mAU)	
2	120676.25±938.58	0.77	118985.56±958.35	0.82
8	792625.05±7825.44	0.98	786565.35±7685.12	0.97
16	1887515.30±12568.40	0.66	1946213.33±11512.31	0.58

Repeatability and intermediate precision (intra-day and inter-day) experiments were conducted to assess the precision of the HPLC method at various concentrations of the working standard solution (6, 10, and 14 µg/mL). The percentage RSD value from the repeatability analysis was determined to be 1.374% (Table 5.10).

Table 5.11 summarizes the results of the intermediate precision studies. The percentage RSD values for the DHA peak area in intra-day precision studies ranged from 0.54 to 1.03%, while the inter-day precision studies showed percentage RSD values ranging from 0.57 to 0.95%.

LOD and LOQ

The LOD and LOQ values for DHA determination were found to be 0.136 µg/mL and 0.979 µg/mL, respectively. The low LOD and LOQ values demonstrate the HPLC method's high sensitivity for DHA analysis.

Robustness

The robustness measures the HPLC technique's ability to withstand small but deliberate changes in method variables, indicating its reliability under typical operating conditions. The robustness and ruggedness of the established HPLC method were evaluated through intentional modifications across various chromatographic settings. The results showed reduced percentage RSD values (<2%) for both area and retention time (Table 5.12), confirming the method's robustness.

Table 5.12 Robustness and ruggedness study of developed HPLC method for DHA (10 µg/ml)

Parameters	Variations made	Area±SD (mAU)	RSD (%)	Retention time (RT)±SD (min)	RSD (%)
Wavelength	264	113573.43±1391.38	1.22	3.59±0.02	0.55
	266	111641.47±1276.38	1.14	3.69±0.03	0.81
	268	118525.14±948.13	0.79	3.87±0.05	1.29
Run time (min)	8	108256.76±1190.44	1.09	3.68±0.04	1.08
	10	115654.84±1253.33	1.08	3.84±0.05	1.30
	12	129773.61±1214.81	0.93	3.76±0.06	1.59
Flow rate (mL/min)	0.8	118182.45±1068.75	0.90	3.89±0.04	1.02
	1	109021.84±1252.05	0.90	3.90±0.03	0.81
	1.2	110190.69±992.65	0.96	3.67±0.05	1.36
Mobile phase composition (Methanol: Water)	78:22	103237.66±895.68	0.75	3.41±0.03	0.87
	80:20	118018.28±787.52	0.65	3.68±0.04	1.08
	82:18	102149.95±1246.31	1.04	3.42±0.04	1.16

5.4.2 Isolation and immunoblotting analysis

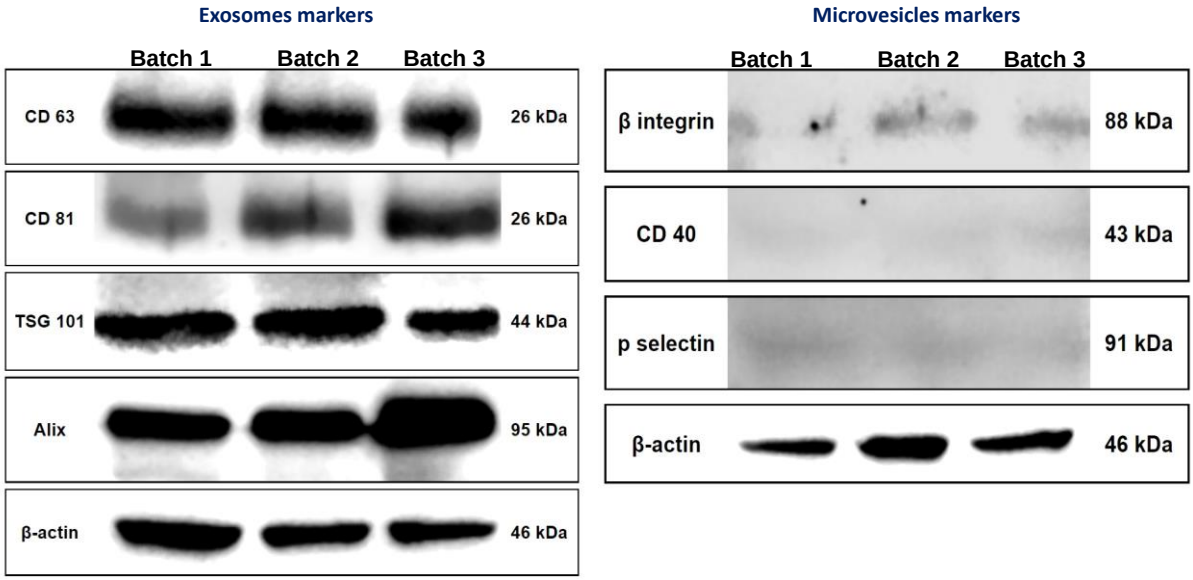

Figure 5.12 Exosomes were isolated in three batches via ultracentrifugation, and purity was confirmed via exosomal and microvesicle biomarkers.

Western blot analysis was utilized to confirm the preparation of exosome protein lysates and verify the presence of key exosomal membrane markers such as CD63, CD81, Tsg101, and Alix (Figure 5.12). The absence of p-selectin, CD40, and β-integrin β1 on the vesicle surface indicated their purity, free from other multivesicular bodies [174].

5.4.3 Isolation and characterization of exosomes and DHA-loaded exosomes

Bovine milk exosomes exhibited an average size, PDI, and zeta potential of 91.8±3.1 nm, 0.135±0.005, and -22.6±0.9 mV, respectively, while the DHA-loaded exosomes (Exo-DHA) showed an average particle size, PDI, and zeta potential of 101.7±2.3 nm, 0.124±0.003, -28.6±0.8 mV respectively (Figure 5.13, C, F, G, H). The change in the particle size suggests that the drugs are successfully loaded within the Exo; however, the change in size was found to be insignificant, and the results are consistence with the previous reports [184]. The zeta potential of Exo-DHA (-28.6±0.8) was found to be more negative, compared to naïve exosomes (-22.6±0.9), indicating excellent stability of both Exo and Exo-DHA. The changes in the zeta potential are due to the binding or attachment of DHA molecules on the surface of exosomes via hydrogen bonding or simple ionic interactions. Further, the % drug loading and % encapsulation efficiency were found to be 16.6±1.1 and 72.9±1.6, respectively (Table 5.9). The surface morphology of Exo and Exo-DHA was confirmed by SEM and AFM (Figure 5.13 A-B, D-E). The morphology revealed that both Exo and Exo-DHA are spherical, and their size obtained from the microscopy was somewhat smaller (approximately 80 nm) than that found from the particle size analyzer. Such variation in the size measurement was observed because the particle size analyzer measures the hydrodynamic size. In contrast, the SEM and AFM measure the actual size of the single entity in the real-time frame. Moreover, the shape of the exosomes remained unchanged even after the loading of DHA, which indicated the exosomes are a suitable vehicle for the delivery of DHA.

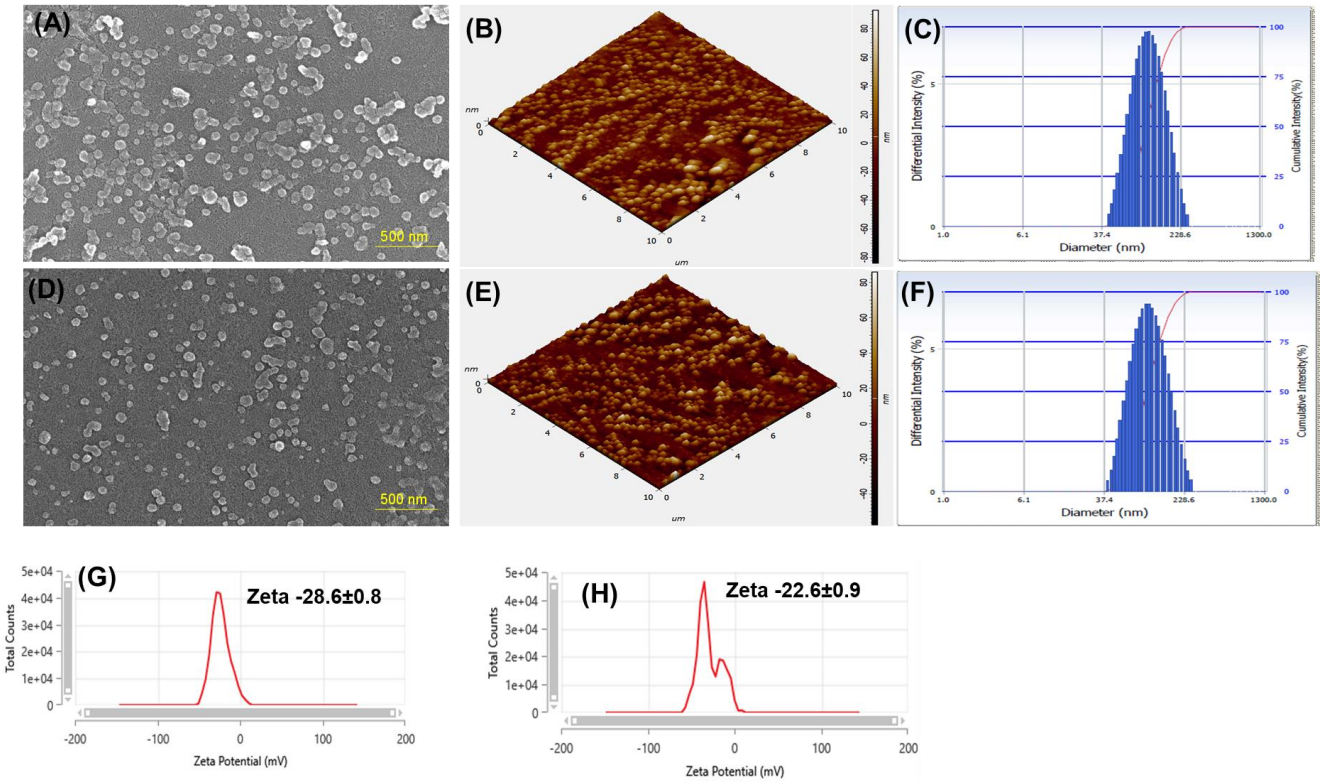

Figure 5.13 Morphology, size, and zeta potential of exosomes and DHA-loaded exosomes: (A-C) Morphology by SEM, AFM, and Size by particle size analyzer of exosomes; (D-E) Morphology by SEM, AFM, and Size by particle size analyzer of Exo-DHA.

Table 5.13 Particle size, PDI, zeta potential, encapsulation efficiency, and drug loading of exosomes and DHA-loaded exosomes

Formulation	Size (nm)	PDI	Zeta potential (ζ)	EE%	DL%
Exo	91.8±3.1	0.135±0.005	-22.6±0.9	-	-
Exo-DHA	101.7±2.3	0.124±0.003	-28.6±0.8	72.9±3.6	18.6±1.1

5.4.4 Optimization of DHA-loaded exosomes

The BBD-enabled optimization analysis offered a second-order quadratic polynomial model. From the ANOVA (Table 5.10 and Table 5.11), the p-value of the model was <0.05, which inferred that the model obtained was analytically significant. Table 5.5 enlists the responses obtained from the BBD. The R2 values for these models ranged between 0.9654 and 0.9753, representing an excellent fit of the quadratic model ($p < 0.05$). Also, the models for the responses showed an insignificant ‘‘lack of fit’’ justifying the suitability of the proposed model.

Table 5.14 BBD with independent variables (factors) and the experimental response for the process optimization

Run	Factor 1 A: Amount of Exo (mg)	Factor 2 B: Amount of drug (mg)	Factor 3 C: Sonication time (sec)	Response 1 Particle size (nm)	Response 2 PDI NA	Response 3 % EE	Response 4 % DL
1	1	10	120	320	0.211	72	16
2	5.5	10	60	142.6	0.167	74	13.25
3	10	10	120	120	0.238	57	10
4	5.5	5.5	120	190	0.342	65.2	15.7
5	5.5	5.5	120	173	0.319	68	13.2
6	10	1	120	103	0.211	79	23
7	5.5	5.5	120	180	0.316	67.7	15.2
8	5.5	10	180	340	0.288	65	8.97
9	5.5	1	60	265	0.321	67.1	5.11
10	5.5	5.5	120	167	0.343	65.4	13.6
11	1	1	120	322	0.372	44.9	6.98
12	10	5.5	180	132	0.254	56	21
13	5.5	5.5	120	190	0.342	65.2	15.7
14	5.5	1	180	179	0.250	58	21.9
15	10	5.5	60	180	0.178	68.9	9.4
16	1	5.5	60	274	0.267	59.7	5.78
17	1	5.5	180	389	0.301	56.8	17

Table 5.15 Analysis of Variance (ANOVA) testing results of the models

Model	**p-value of model**	**R^2**
Particle size	< 0.0001	0.9754
PDI	< 0.0001	0.9654
Encapsulation efficiency	< 0.0001	0.9658
Drug loading	< 0.0001	0.9753

Figure 5.14 (A)–5.14 (C) presents the 3D response surface plot for particle size. The results indicate that increasing sonication time and reducing drug concentration lead to a significant decrease in particle size. This effect is likely due to enhanced mechanical stress and reduced drug loading. Conversely, an increase in exosome concentration results in a larger particle size, possibly due to the higher total lipid content.

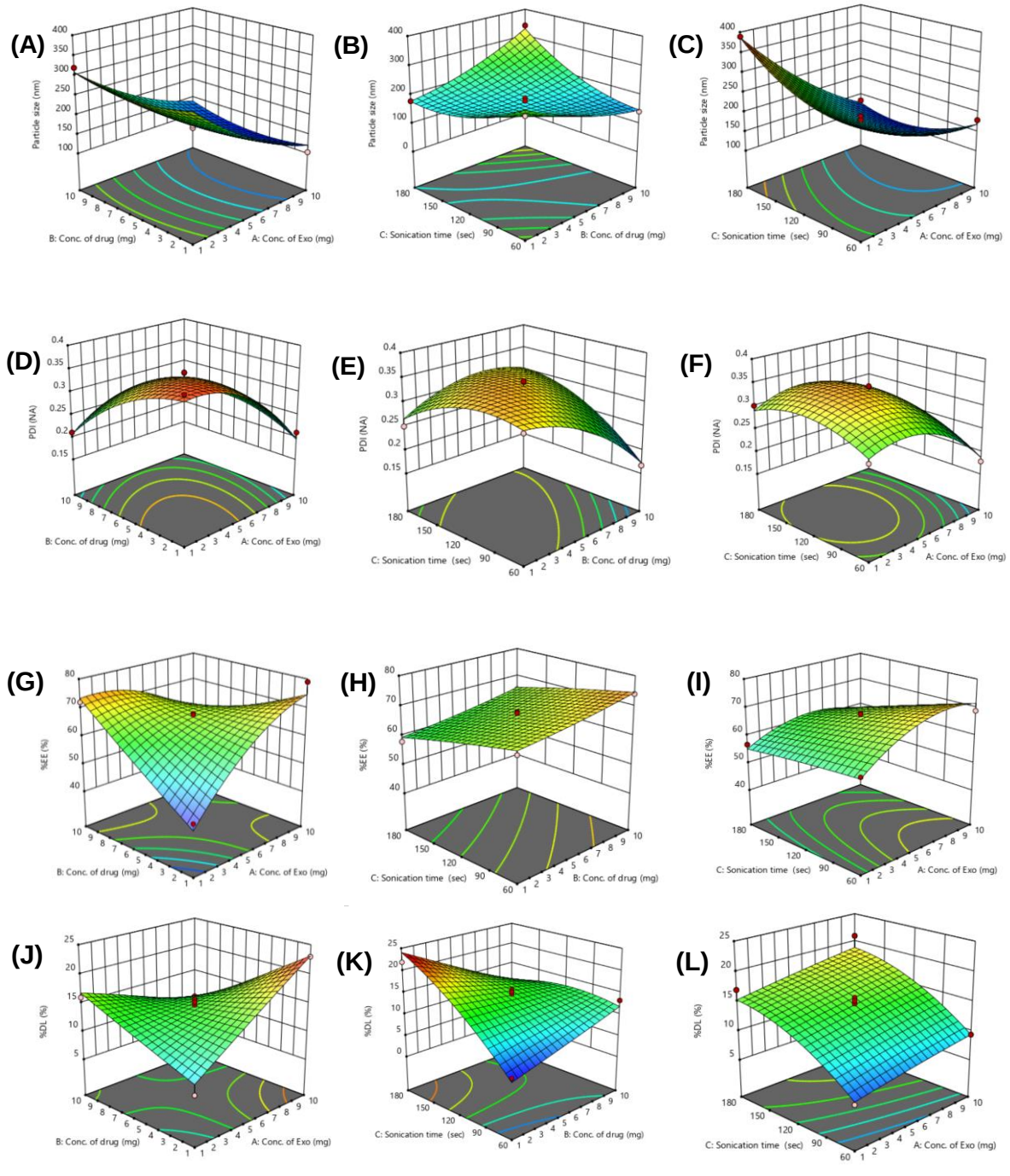

Figure 5.14 3D response surface plots indicating the interaction of the independent variables on particle size (A-C), PDI (D – F), % encapsulation efficiency (G – I), and % drug loading (J – L).

Figure 5.14 (D)–5.14 (F) demonstrates that both the drug concentration and exosome concentration negatively impact the PDI across all levels. Additionally, a reduction in PDI was observed with increased sonication time, indicating improved uniformity in particle size distribution at higher sonication levels.

Figure 5.14 (G)–5.14 (I) illustrates that increasing the concentration of both the drug and exosomes leads to a corresponding increase in encapsulation efficiency. However, sonication time does not significantly affect encapsulation efficiency. Similar trends were observed for drug loading (%), as shown in Figure 5.14 (J)–5.14 (L), where higher drug and exosome concentrations resulted in increased drug loading, with sonication time having no noticeable impact.

Moreover, the residual plots obtained were found to be quite regulated, with narrow distribution and random scattering around the zero-axis, as shown in Figure 5.15 (A – D).

From the BBD, the optimum exosomal formulation was obtained, consisting of 9 mg exosomes, 1 mg drug, and 120 sec of sonication time, which overall gave the desirability value of 1.000 and falls within a 95% prediction interval (α = 5%).

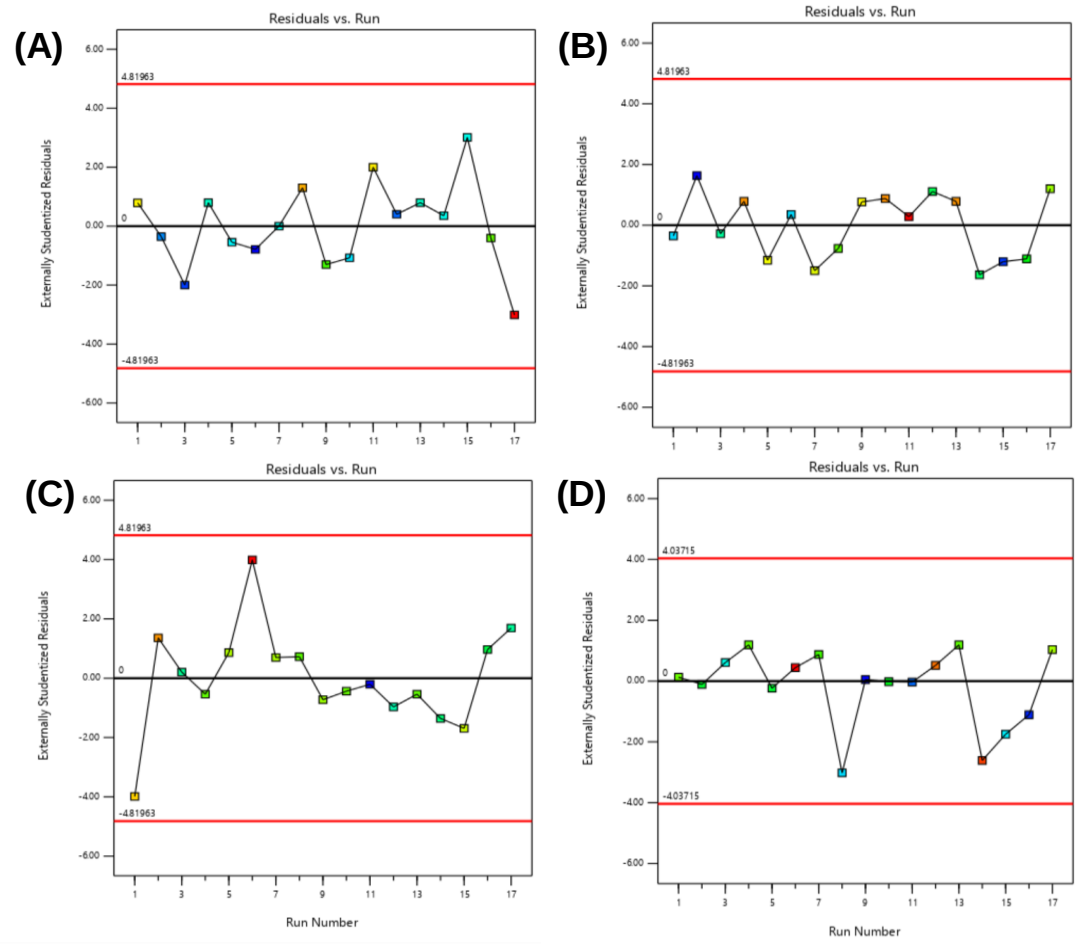

Figure 5.15 Residual plots showing the run distribution for particle size (A), PDI (B), % encapsulation efficiency (C), and % drug loading (D).

5.4.5 X-Ray diffraction

The X-ray diffraction pattern of DHA, Exo, and Exo-DHA was determined. As shown in Figure 5.16 (A), a single peak was noticed at 31.62º in the case of exosomes, illustrating the crystalline nature of the Exo. DHA also depicts its crystalline nature by showing several sharp peaks at 11.16°, 12.31°, 16.74°, 17.48°, 19.23°, 19.99°, and 30.01°. In the case of Exo-DHA, the characteristic peaks of Exo and DHA were observed at 10.96°, 12.15°, 18.45°, and 31.55°. However, not all characteristic peaks of DHA were observed in DHA-loaded exosomes; also, some of the peaks were shown with low intensity with minor changes in the theta values. It was inferred that the slight changes in 2theta and disappearance of some peaks are due to the binding of the DHA to the exosomal surface through hydrophobic interaction and changes in their binding energy.

5.4.6 Stability study

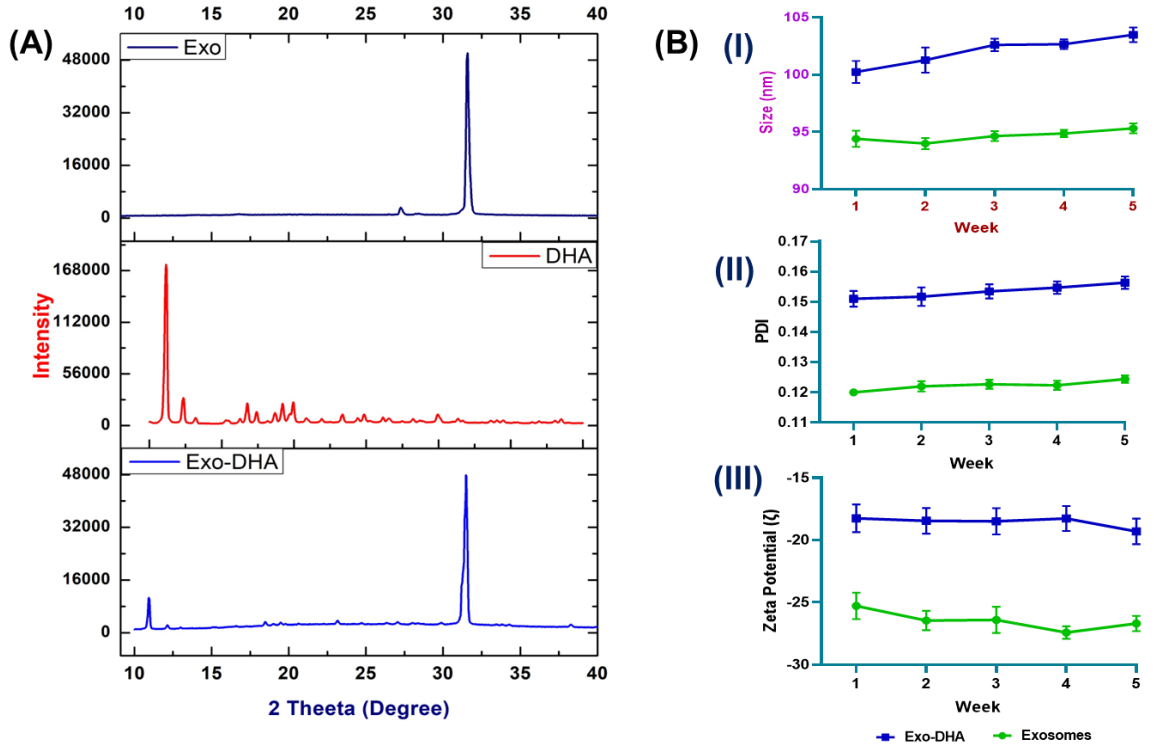

Figure 5.16 XRD and stability of Exo and Exo-DHA, (A) represent XRD of Exo, DHA, and Exo-DHA, (B) stability of exosomes when stored in refrigerated conditions for different times in terms of the effect on (I) particle size, (II) PDI, (III) zeta potential.

The stability of exosomes and Exo-DHA were investigated in terms of particle size, PDI, and zeta potential by storing them at frozen condition (-80ºC) for 1 month (5 weeks). Figure 5.16 (B) shows insignificant changes in the particle size of Exo and DHA-loaded Exo. Similar results were observed in the case of PDI and zeta potential. The insignificant changes in the analyzed parameters indicated that exosomes are stable in refrigerated conditions for a short period. However, a long stability status followed by the investigation of drug and exosome content is required for further confirmation of the stability of exosomes.

5.4.7 Drug release

The *in vitro* release profile of DHA and Exo-DHA was performed in two different pH conditions viz., pH 7.5 to mimic blood condition and pH 5.5 to mimic the tumor microenvironment. As shown in Figure 5.17, a biphasic release profile was observed in the case of Exo-DHA, while DHA showed continuous release, where the total drug gets released within 6 h in both pH conditions. In the case of Exo-DHA, a burst release was noticed in the initial 1 hour, where almost 20% of DHA was released from exosomes in both pH conditions, followed by a sustained release for up to 48 h where 87% of DHA was released from exosomes at pH 7.4, while 98% was released at pH 5.5. The difference in release patterns is due to the binding of some part of the drug on the surface of exosomes via hydrophobic interactions or the formation of hydrogen bonding which offers burst release. In contrast, the sustained release was due to the diffusion of DHA encapsulated within the exosomes. It was further inferred that the dual release pattern of the DHA from exosomes could be helpful in the inhibition of tumor proliferation in both short and long-term treatment. Moreover, it was concluded that more concentration of drugs gets released in pH 5.5 because it mimics the acidic tumor microenvironment where the presence of many proteins and peptidoglycan could rupture the exosomal membrane and be helpful in the higher drug release [193].

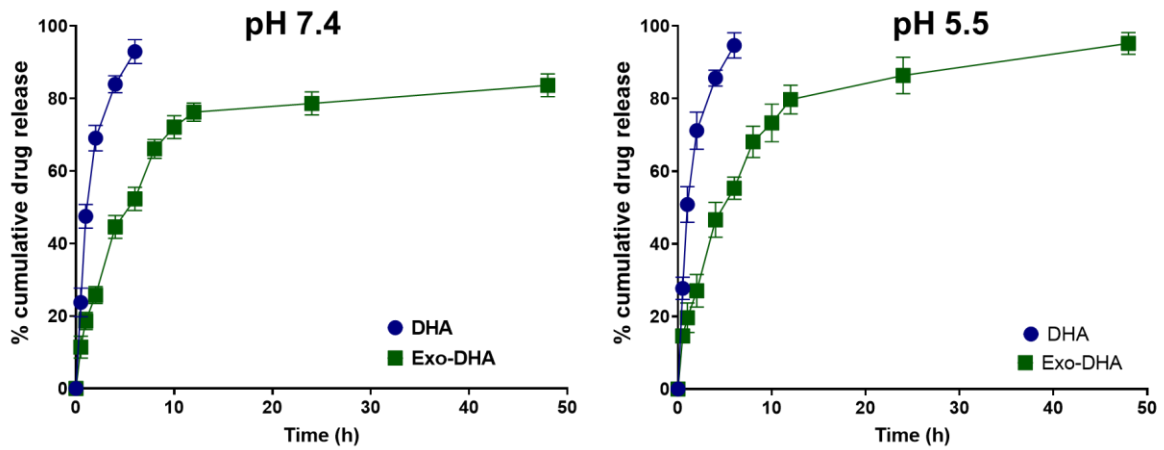

Figure 5.17 Drug release for DHA and Exo-DHA was performed at pH 7.4 (A) and pH 5.5 (B) via the dialysis bag method. pH 7.4 mimics the blood condition, and pH 5.5 mimics the tumor environment.

5.4.8 Cytotoxicity study

The cytotoxicity assay is a primary experimental setup to detect developed molecules' anticancer properties

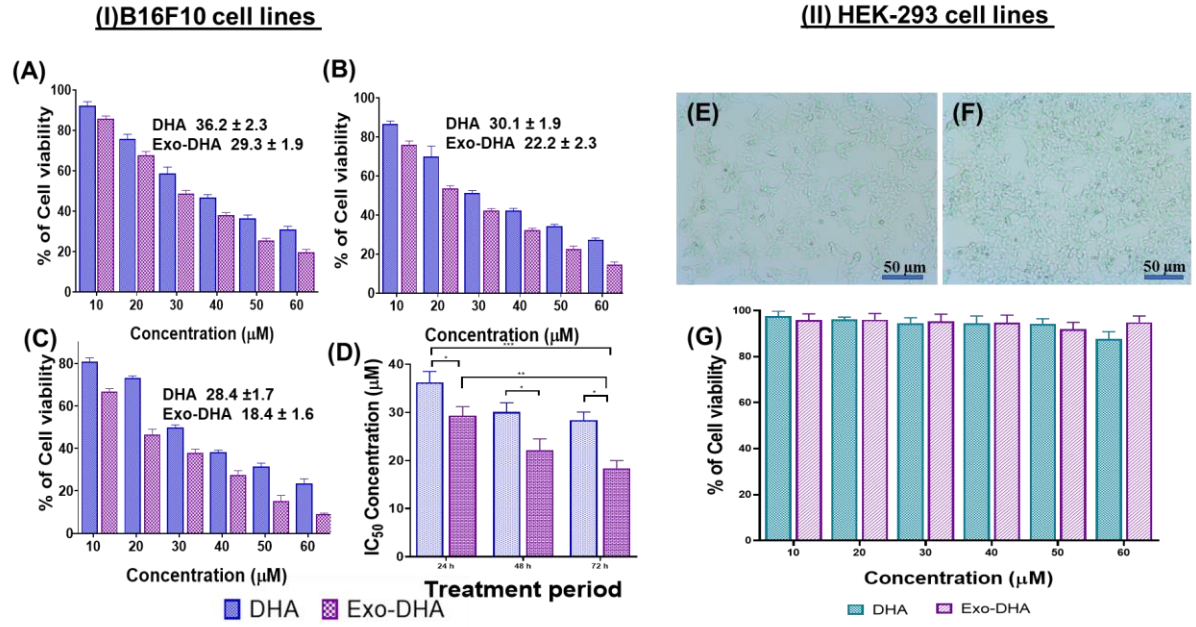

Figure 5.18 Cytotoxicity of DHA and Exo-DHA in (I) B16F10 cell lines, and (II) HEK-293 cell lines for 24, 48, and 72 h. Statistical analysis was performed by One-Way ANOVA followed by the Tukey P test with multiple comparisons and the level of significance *$p < 0.05$, **$p < 0.01$, and ***$p < 0.001$.

. In the present study, the cytotoxicity and safety of DHA were investigated in B16F10 and HEK-293 cell lines, respectively. In this study, if the cells are alive, they will convert the MTT

to insoluble purple formazan crystals, and if dead, no such crystal formation occurs. Hence, it could be inferred from the observation that the production of color is directly proportional to cell viability. As shown in Figure 5.18 (A-D), an MTT assay was performed for 24, 48, and 72 h, and the IC50 of DHA and Exo-DHA was found to be 36.2±2.3 and 29.3±1.9, respectively, after 24 h treatment. The IC50 values were significantly reduced after 48h, and the IC50 of DHA and Exo-DHA were found to be 30.1±1.9 and 22.2±2.3, respectively. Similar results were found after 72 h treatment.

5.4.9 Qualitative cell uptake assay

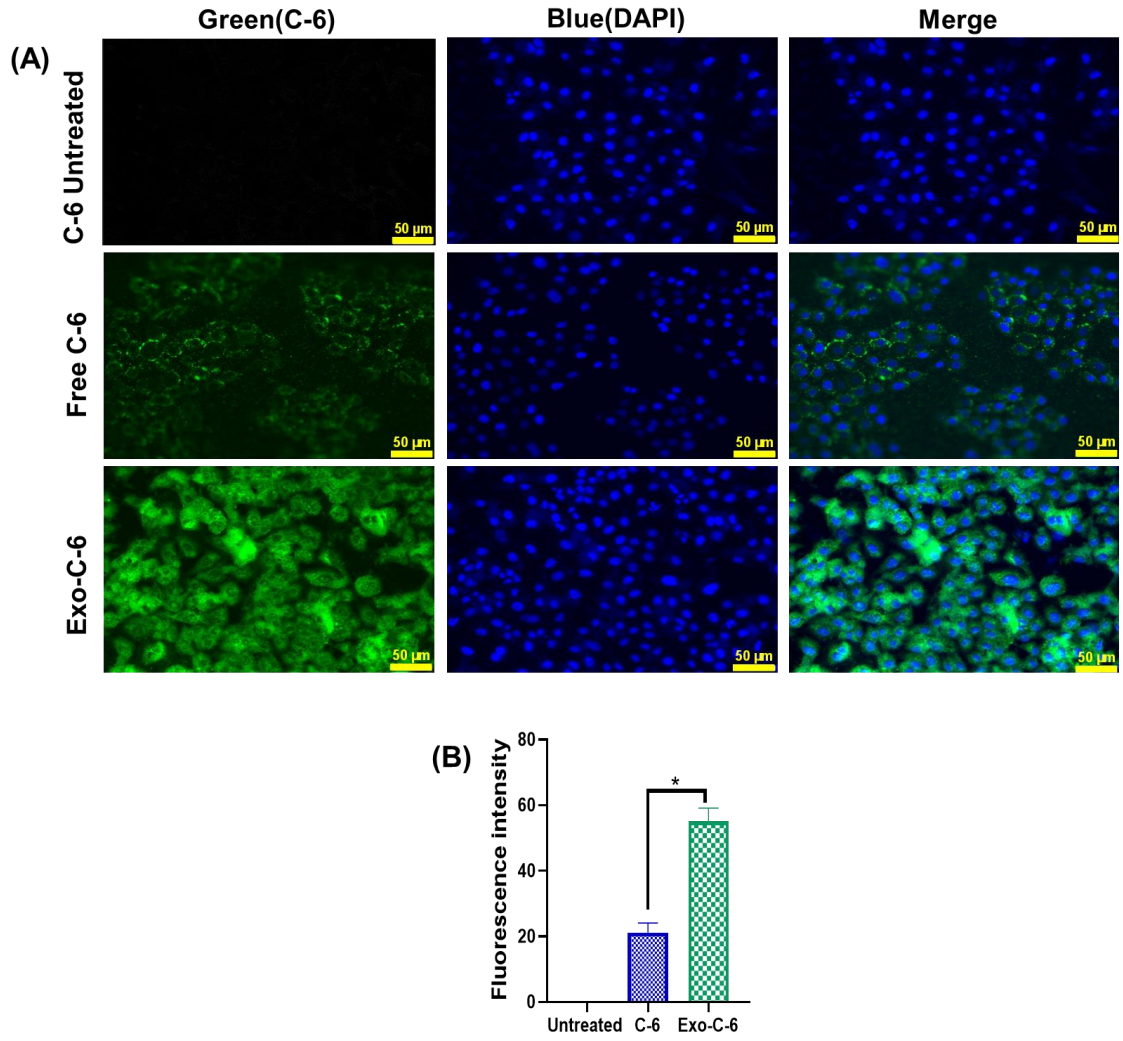

Figure 5.19 Qualitative cellular uptake of Coumarin-6 and Coumarin-6 loaded exosomes in B16F10 cell lines. Cells were observed in the green channel for C-6 and the blue channel for DAPI. Statistical analysis was performed by One-Way ANOVA followed by the Tukey P test with multiple comparisons and the level of significance *$p < 0.05$.

An intracellular uptake assay was performed to check the internalization capability of exosomes into the cancerous cells. DHA is not a fluorescent molecule and cannot produce fluorescence; hence it is substituted by coumarin-6 (C-6). The dye-loaded exosomes (Exo-C-6) were used to study the intracellular uptake.

C-6 is a lipophilic dye and mimics the DHA property. As shown in Figure 5.19, the green fluorescence was significantly higher in the Exo-C-6 as compared to free C-6. In contrast, the cells with no green fluorescence were observed in the C-6 untreated group, indicating that green fluorescence is due to the C-6 uptake. Moreover, the DAPI was used to stain the nucleus, and from the results, it was observed that the C-6 was found inside the cells rather than the cell's surface. Moreover, the intracellular uptake results were found consistent with previous reports [194].

5.4.10 Apoptosis assay by 4,6-Diamidino-2-phenylindole (DAPI) staining

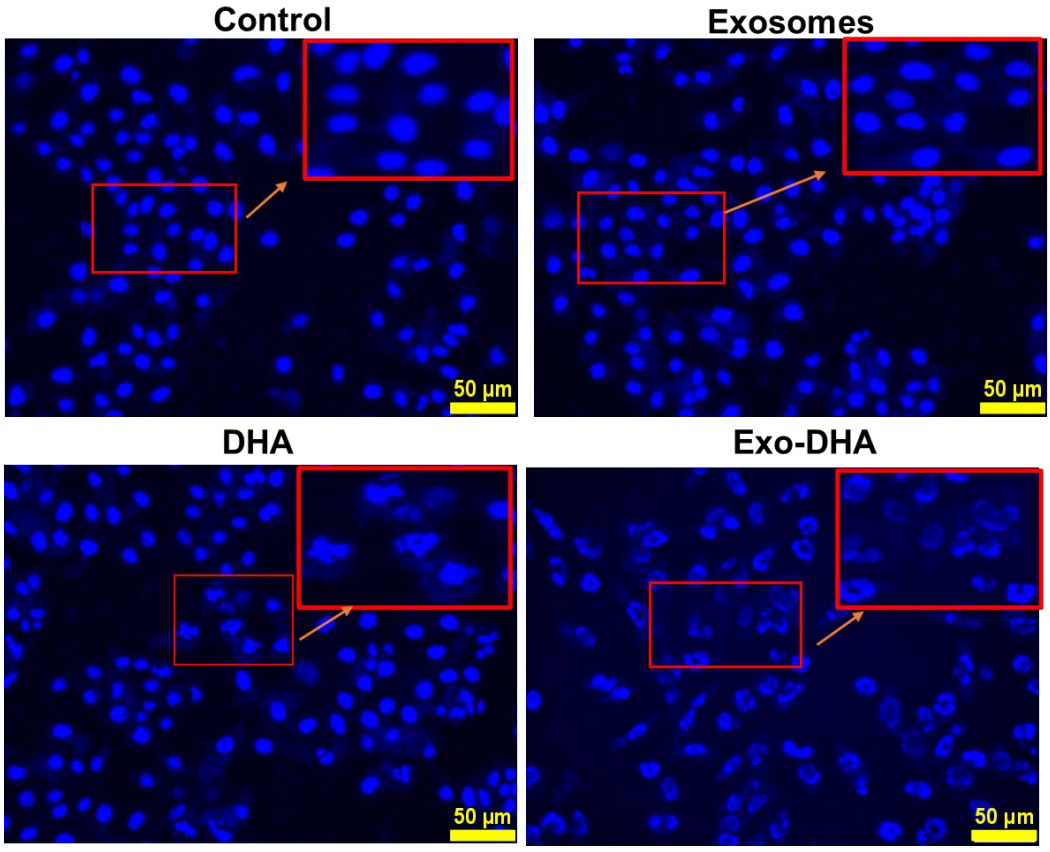

Figure 5.20 Nuclear DNA fragmentation assay performed with DAPI staining.

DHA induces apoptosis in cancer cells via intrinsic (external death receptor) and extrinsic (via the nucleus) pathways. In the nuclear fragmentation assay, the intrinsic apoptosis pathway was measured by staining the nucleus with nuclear DAPI, and morphological changes were observed, such as the condensed or fragmented nuclei and horseshoe-shaped nuclei. As shown in Figure 5.20, the shape of the nuclei treated with Exo-DHA was changed (fragmented, disoriented structure) compared to the nuclei of the control and DHA groups. The results indicated that the DHA produces apoptosis via an intrinsic pathway, and these findings are in accordance with previous reports [148].

5.4.11 Apoptosis assay

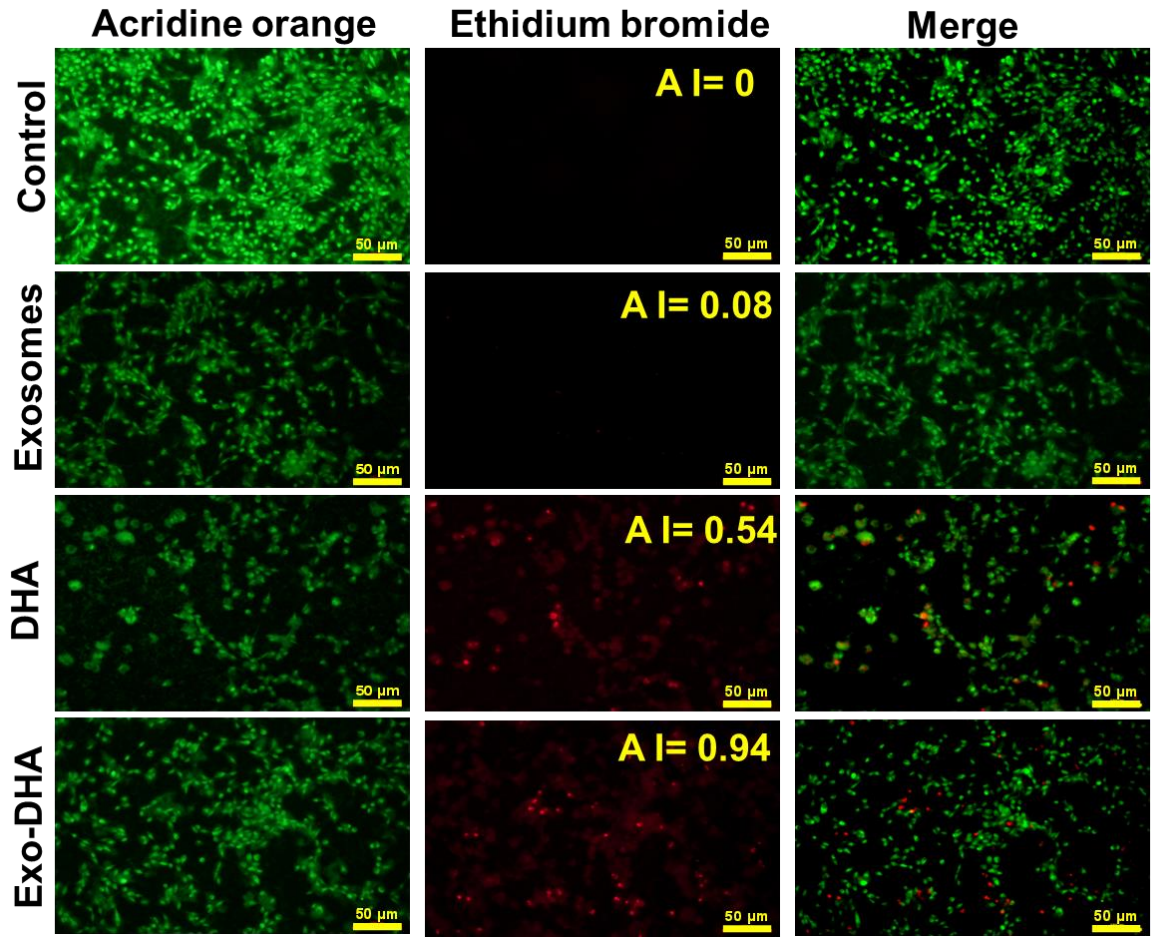

Figure 5.21 Apoptosis assay was performed by acridine orange/ethidium bromide in B16F10 cell lines. Acridine orange binds to the live cells, while ethidium bromide binds to the dead cells. AI: Indicates the apoptotic index.

The induction or enhancement of intracellular apoptosis is a critical mechanistic pathway for many anti-cancer drugs, including DHA. Therefore, we conducted an apoptosis assay using acridine orange and ethidium bromide staining to support our hypothesis.

Acridine orange is a nuclear stain that penetrates both live and dead cell nuclei, binds to DNA through intercalation, and emits green fluorescence. In contrast, ethidium bromide is a non-permeable dye that emits red fluorescence after binding to the DNA of dead cells [186]. As depicted in Figure 5.21, cells treated with Exo-DHA exhibited more dead cells than those treated with DHA alone. Furthermore, we calculated the apoptotic index (AI), which was found to be higher in Exo-DHA-treated cells (0.94) than in DHA-treated cells (0.54). This finding indicates that the *in vitro* efficacy of DHA was enhanced when loaded into exosomes.

5.4.12 Reactive oxygen species assay

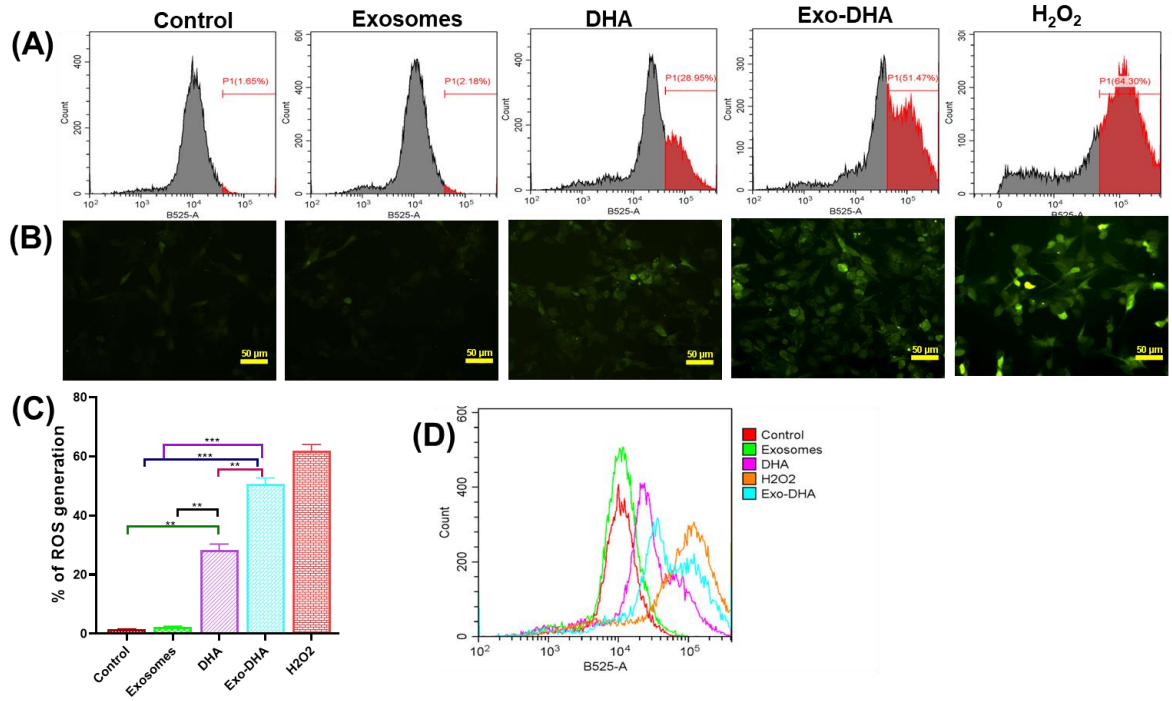

Figure 5.22 Reactive oxygen species assay by flow cytometry (A), and fluorescence microscopy (B). After the treatment cells were incubated with H2DCFDA dye. Statistical analysis was performed by One-Way ANOVA followed by the Tukey P test with multiple comparisons and the level of significance $^{**}p < 0.01$ and $^{***}p < 0.001$.

Low production of ROS in the normal cells leads to the growth of cancer, although the generation of a high amount of ROS in cancer leads to the cancer cell's death. It was observed from various literature surveys that many anticancer drugs, including DHA, produce ROS as a mechanistic approach to cancer cell death. DHA contains an endoperoxide bridge, which cleaves in the presence of stimuli, and free radicals (reactive oxygen species) are generated via the Fenton reaction [195].

As shown in Figure 5.22, the assay was performed via fluorescence microscope (Figure 5.22 B) and flow cytometry (Figure 5.22 A and D), where the result indicated that the Exo-DHA significantly produced a high amount of ROS compared to DHA. The cells with plain media were considered as the negative control while the cells treated with H2O2 were taken as the positive control. Moreover, our results are in accordance with the reported results [146].

5.4.13 Mitochondrial membrane potential assay

It is widely recognized that mitochondria are the "powerhouse" of cells, indicating any cell's health status. According to observations, the loss of mitochondrial membrane potential (MMP) causes the contents of the mitochondria to leak into the cell's cytoplasm, which in turn triggers the early stages of apoptosis or cell death [196]. The cationic membrane-permeant JC-1 dye is frequently used to track the health of the mitochondria. When the cell is healthy, a high accumulation of JC-1 occurs inside the mitochondria due to the membrane potential and emits red fluorescence. However, during apoptosis, the membrane potential is disrupted, causing the JC-1 dye to dissociate and emit green fluorescence [197].

As shown in Figure 5.23, the formation of JC-1 aggregates decreases in Exo-DHA, as compared to DHA, as evident from the fluorescence intensity ($p < 0.05$), which was calculated via image J software (Figure 5.23, B). Hence, it was inferred that DHA exerts anticancer activity by decreasing the mitochondrial membrane potential.

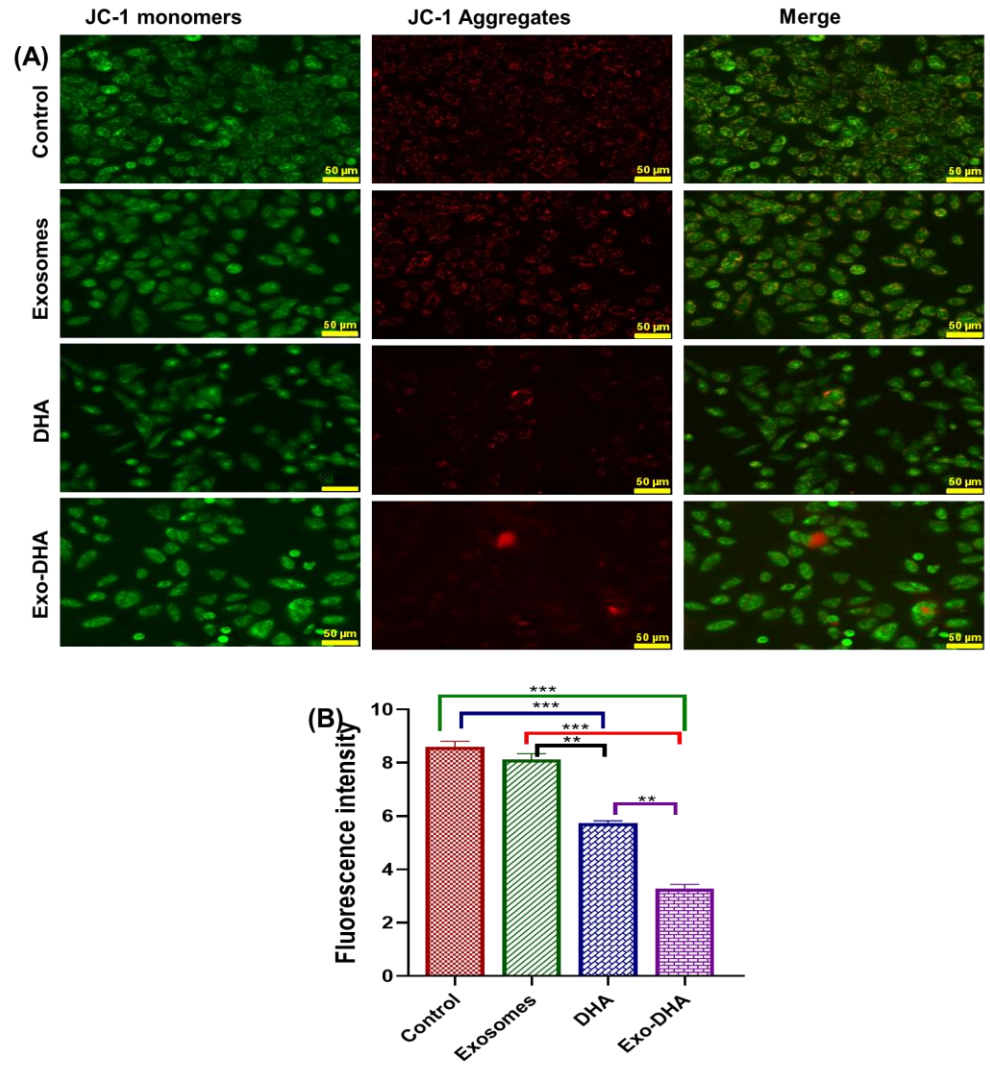

Figure 5.23 Mitochondrial membrane potential assay, green fluorescence indicates JC-1 monomers and red fluorescence indicates the J-aggregates. Statistical analysis was performed by One-Way ANOVA followed by the Tukey P test with multiple comparisons and the level of significance $^{**}p < 0.01$ and $^{***}p < 0.001$.

5.4.14 Colony formation assay

The formation of cell colonies after the treatment via chemotherapy or radiation therapy is an essential characteristic of cancer recurrence. The effect of drugs or developed formulations on colony formation was investigated via colony formation or clonogenic assay [196]. As shown in Figure 5.24, the formation of cell colonies is significantly higher in DHA treated group ($p < 0.05$) compared to the cells treated with Exo-DHA. The results suggested that the developed Exo-DHA could inhibit cancer recurrence.

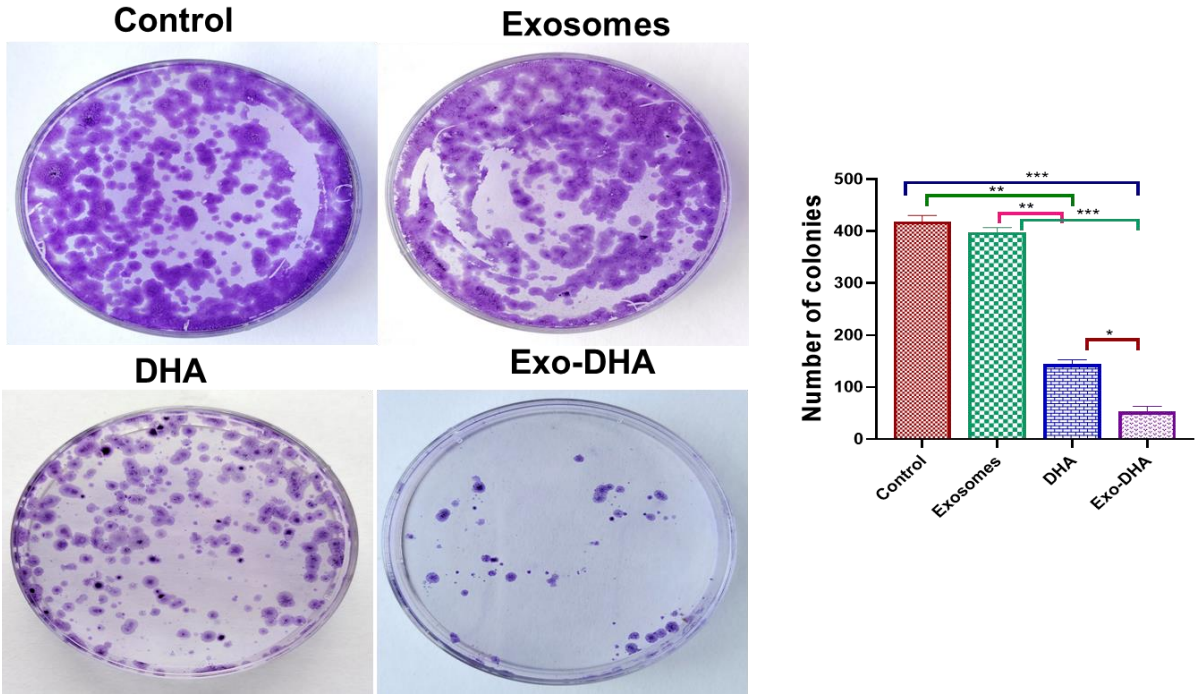

Figure 5.24 Colony formation assay was performed in B16F10 cell lines. Treatment was given with exosomes, DHA, and Exo-DHA. Statistical analysis was performed by One-Way ANOVA followed by the Tukey P test with multiple comparisons and the level of significance *$p < 0.05$, **$p < 0.01$ and ***$p < 0.001$.

5.4.15 Cell migration assay

Compared to all skin cancers, melanoma is the most aggressive and has high metastasis capability, mainly to the lungs and bone marrow. In melanoma, metastasis occurs due to the lack of oxygen and nutrient supply, escape from the attack of the immune cells, and triggering some metastatic factors [197]. Hence, we have performed a transwell migration assay and wound healing assay to investigate whether DHA and Exo-DHA can inhibit cell migration in melanoma. As shown in Figure 5.25, the control and DHA-treated groups have shown significant migration compared to Exo-DHA-treated groups ($p < 0.05$). The inhibition of cell migration could be due to the regulation of Epithelial-Mesenchymal Transmission (EMT) - regulated genes such as Slug, ZEB1, ZEB2, and Twist and downregulation of expression of Snail and PI3K/AKT Signalling pathway [198]. Furthermore, DHA reduced the connection between the tumor and the tumor microenvironment and suppressed the transforming growth

factor-β (TGF-β) signaling, which in turn suppressed the activation of cancer-associated fibroblasts (CAFs) and mouse cancer-associated fibroblasts (L-929-CAFs) [199]. In addition, DHA also inhibits cell migration by inhibiting downregulating phosphorylated focal adhesion kinase (pFAK), MMP-2, von Willebrand factor (vWF), and macrophage infiltration. Above all the mechanisms or any one mechanism is responsible for cancer cell migration by DHA [200]. However, further investigation is required to confirm the anti-metastatic properties of DHA and Exo-DHA *in vivo*.

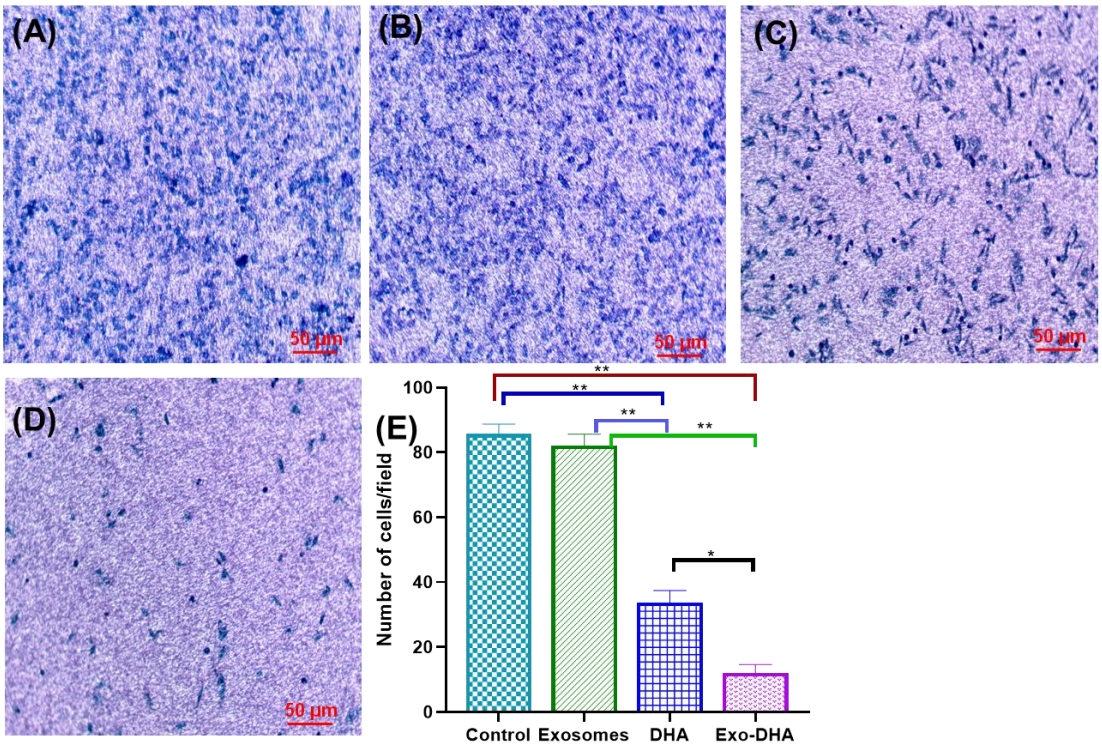

Figure 5.25 Transwell migration assay shows the Exo-DHA significantly reduces the migration of B16F10 cell lines. (A) represents control, (B) treated with exosomes, (C) treated with DHA, (D) treated with Exo-DHA. (E) Statistical analysis was performed by One-Way ANOVA followed by the Tukey P test with multiple comparisons and the level of significance *$p < 0.05$, **$p < 0.01$.

5.4.16 Wound healing assay

Like the transwell migration assay, wound healing assay was employed to confirm further the anti-metastatic properties of DHA and Exo-DHA in B16F10 cell lines. As shown in Figure

5.26, the healing of wounds is significantly decreased in Exo-DHA compared to the DHA-treated cells.

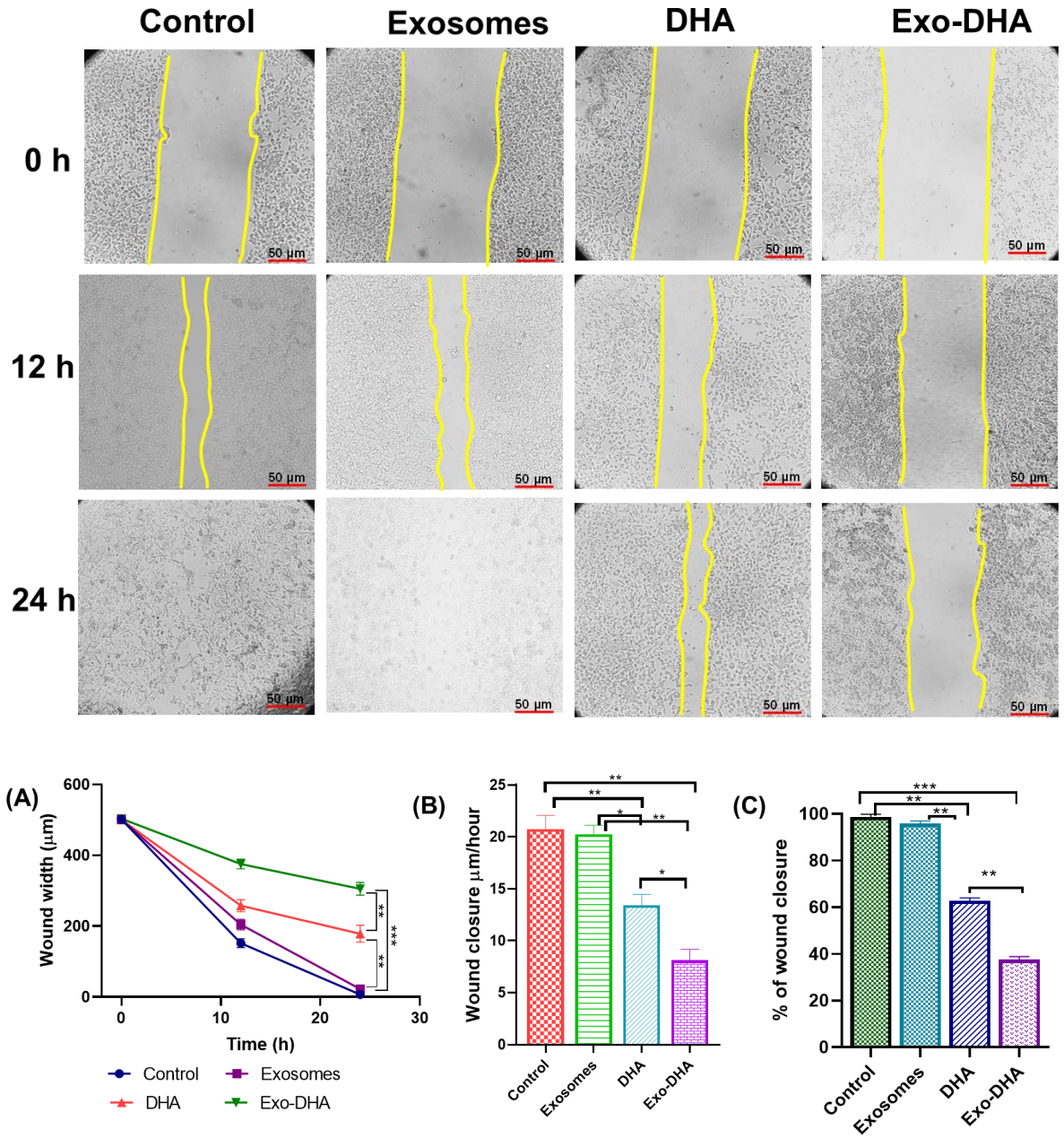

Figure 5.26 Wound healing assay was performed in B16F10 cell lines and healing was observed at 0, 12, and 24 h. Exo-DHA significantly inhibited the migration of the cells compared to DHA. The percent of wound healing is calculated via the (A) wound width with respect to time and (B) wound closure (µm/hour), (C) % of wound closure. Statistical analysis was performed by One-Way ANOVA followed by the Tukey P test with multiple comparisons and the level of significance *$p < 0.05$, **$p < 0.01$ and ***$p < 0.001$.

Furthermore, the % of wound closure was significantly ($p < 0.001$) low in Exo-DHA-treated cells compared to control and DHA-treated cells (Figure 5.26 C). Moreover, the rate of wound

closure per hour is significantly low in Exo-DHA. All the *in vitro* results suggested that exosomes significantly improved the anticancer efficacy of DHA. However, further *in vivo* investigations are indispensable to confirm its efficacy.

5.4.17 Immunoblotting

It has been reported that DHA induces apoptosis and decreases migration by modifying cellular signaling pathways such as Bcl-2, Bax, AKT, STAT-3, Survivin, Caspases, and MMP proteins [201]. To prove the improved efficacy of DHA with exosomes at cellular levels, we have performed western blotting analysis for different apoptotic, anti-apoptotic, and migration initiative proteins such as Bax, BCl-2, survivin, and MMP-9. From the results, it was found that the expression level of anti-apoptotic proteins such as Bcl-2 and survivin have significantly ($p < 0.05$) decreased in Exo-DHA as compared to the DHA (Figure 5.27, A-B).

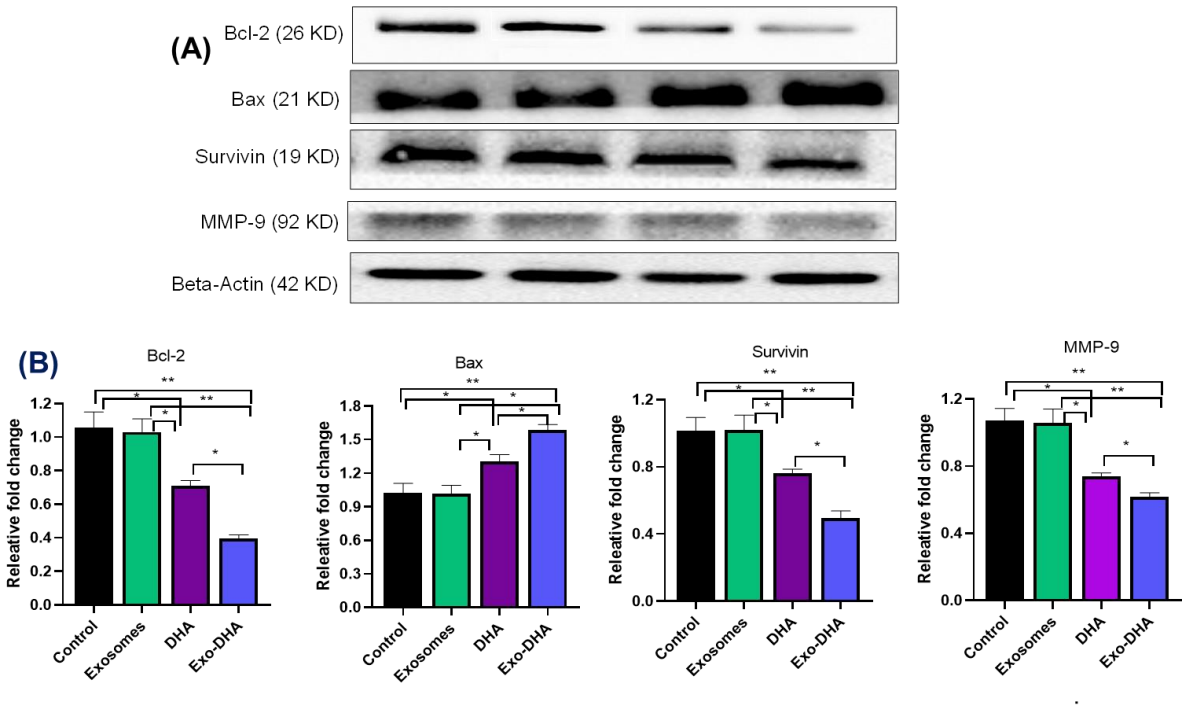

Figure 5.27 Improved anti-cancer efficacy of Exo-DHA *in vitro* was confirmed by western blotting by evaluating apoptotic, and migration proteins. (A) The immune blotting was performed for Bcl-2, Bax, Survivine, and MMP-9. (B) Statistical analysis was performed by One-Way ANOVA followed by the Tukey P test with multiple comparisons and the level of significance *$p < 0.05$, **$p < 0.01$.

While the expression level of apoptotic proteins like Bax has significantly increased in Exo-DHA ($p < 0.05$). The increased expression of apoptotic proteins could be assigned to the generation of free radicles via the Fenton reaction [142]. On the other hand, the expression levels of MMP-9 were significantly ($p < 0.05$) decreased in Exo-DHA compared to DHA. MMP-9 is a metallo matrix protein involved in the migration of cells, and its high expression indicates the metastatic nature of melanoma.

5.4.18 Pharmacokinetics

Before evaluating the efficacy of DHA with exosomes in tumor-bearing mice, it is crucial to assess the oral bioavailability of DHA. Therefore, we initially quantified the oral bioavailability of DHA in SD rats. The mean plasma concentration-time profile of DHA after oral administration of DHA and Exo-DHA is depicted in Figure 5.28 A and the results are summarized in Table 5.12. The plasma concentration of DHA was significantly higher when delivered through Exo-DHA compared to free DHA. Statistical analysis was conducted using one-way ANOVA followed by the Tukey post hoc test, revealing a significant difference between free DHA and Exo-DHA in terms of Cmax and AUC 0-t values. The Cmax of DHA from Exo-DHA (5.431±0.298) was notably higher ($p < 0.01$) compared to free DHA (2.163±0.152), indicating an approximately 2.2-fold increase. Similarly, the area under the curve from time 0 to 24 h (AUC 0-t) of Exo-DHA (42.054±3.871) was significantly ($p < 0.001$) higher, showing a 3.6-fold increase compared to free DHA. Furthermore, the Tmax (time to reach peak plasma concentration) was significantly ($p < 0.01$) improved in Exo-DHA (8 h) compared to free DHA (4 h). The improved bioavailability of DHA with Exo-DHA could be attributed to several factors: i) reduced degradation of DHA in the stomach, ii) enhanced absorption of DHA through exosomes, iii) sustained release of DHA from exosomes, and iv) increased systemic circulation of exosomes [175]. Additionally, the clearance to bioavailability

ratio was decreased in Exo-DHA (0.901±0.004) compared to DHA (3.762±0.124), possibly due to the reabsorption of exosomes into the systemic circulation during filtration.

5.4.19 Tissue distribution

Tissue biodistribution studies were conducted to assess the accumulation pattern of DHA in various organs after oral administration of 50 mg/kg equivalent DHA. Following a 6-hour interval post-administration, the animals were euthanized, and vital organs including the intestine, lungs, liver, heart, kidney, and spleen were collected for quantitative assessment of drug distribution. As illustrated in Figure 5.28 B, the accumulation of free DHA was notably higher in the liver (4.3 µg/g) but comparatively lower in the heart (0.6 µg/g

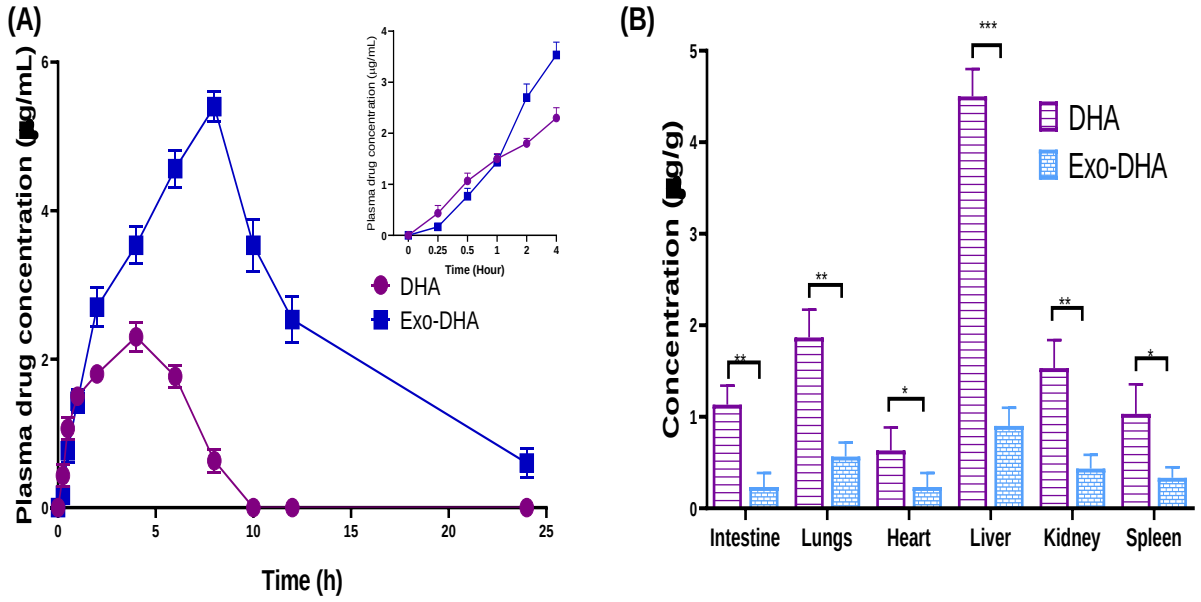

Figure 5.28 Pharmacokinetic profile and tissue distribution of DHA and Exo-DHA after oral administration at 50 mg/kg. (A) represents the pharmacokinetic profile, and (B) tissue distribution. Statistical analysis was performed by One-Way ANOVA followed by the Tukey P test with multiple comparisons and the level of significance *$p < 0.05$, **$p < 0.01$ and ***$p < 0.001$.

). However, in animals treated with Exo-DHA, the concentration of DHA in the liver was significantly reduced ($p < 0.001$). This decrease in liver accumulation of free DHA could be beneficial in mitigating potential liver toxicity associated with high concentrations of the drug in this organ. Conversely, the concentration of free DHA was significantly higher ($p < 0.01$) in

the intestine compared to Exo-DHA-treated animals, which could contribute to the improved oral bioavailability of DHA observed with Exo-DHA formulation. This differential tissue distribution highlights the potential advantages of utilizing exosome-based delivery systems in enhancing drug efficacy while minimizing adverse effects in specific organs.

Table 5.16 Pharmacokinetic parameters of DHA and Exo-DHA after oral administration

PK parameters	**Unit**	**DHA**	**Exo-DHA**
C_{max}	μg/mL	2.163±0.152	5.431±0.298**
T_{max}	h	4	8**
AUC_{0-t}	μg/mL*h	12.325±1.654	42.054±3.871***
$AUC_{0-\infty}$	μg/mL*h	13.289±1.325	55.442±3.184
$t_{1/2}$	h	1.672±0.214	2.362±0.542*
K_e	1/h	0.414±0.004	0.189±0.005
MRT_{0-t}	h	3.894±0.114	6.654±0.125
$MRT_{0-\infty}$	h	4.367±0.164	9.221±0.154
Vz/F	(mg/kg)/(μg/mL)	9.075±0.201	4.766±0.214
CL/F	(mg/kg)/(μg/mL)/h	3.762±0.124	0.901±0.004

Values are represented as mean±SD

C_{max} peak plasma concentration, T_{max} time to reach peak plasma concentration, AUC_{0-t} area under the plasma drug concentration-time curve from time 0 to 24 h, $AUC_{0-\infty}$ area under the plasma drug concentration-time curve from time 0 to infinity h, $t_{1/2}$ elimination half-life, K_e elimination rate constant, MRT_{0-t} mean residence time from time 0–24 h, $MRT_{0-\infty}$ mean residence time from time 0 to infinity h, V_z/F apparent volume of distribution, CL/F apparent systemic clearance following an oral administration $*p < 0.05$, $**p < 0.01$ and $***p < 0.001$ when compared with rats administered with DHA

5.4.20 *In vivo* anti-cancer efficacy study

The anti-cancer efficacy of DHA after loading into exosomes was further validated through an *in vivo* anti-cancer efficacy study conducted in Swiss mice with B16F10-induced melanoma. Tumors were developed by subcutaneously implanting 5 x 10^5 B16F10 cells in mice, and treatment began once the tumor size reached 60-80 mm^3.

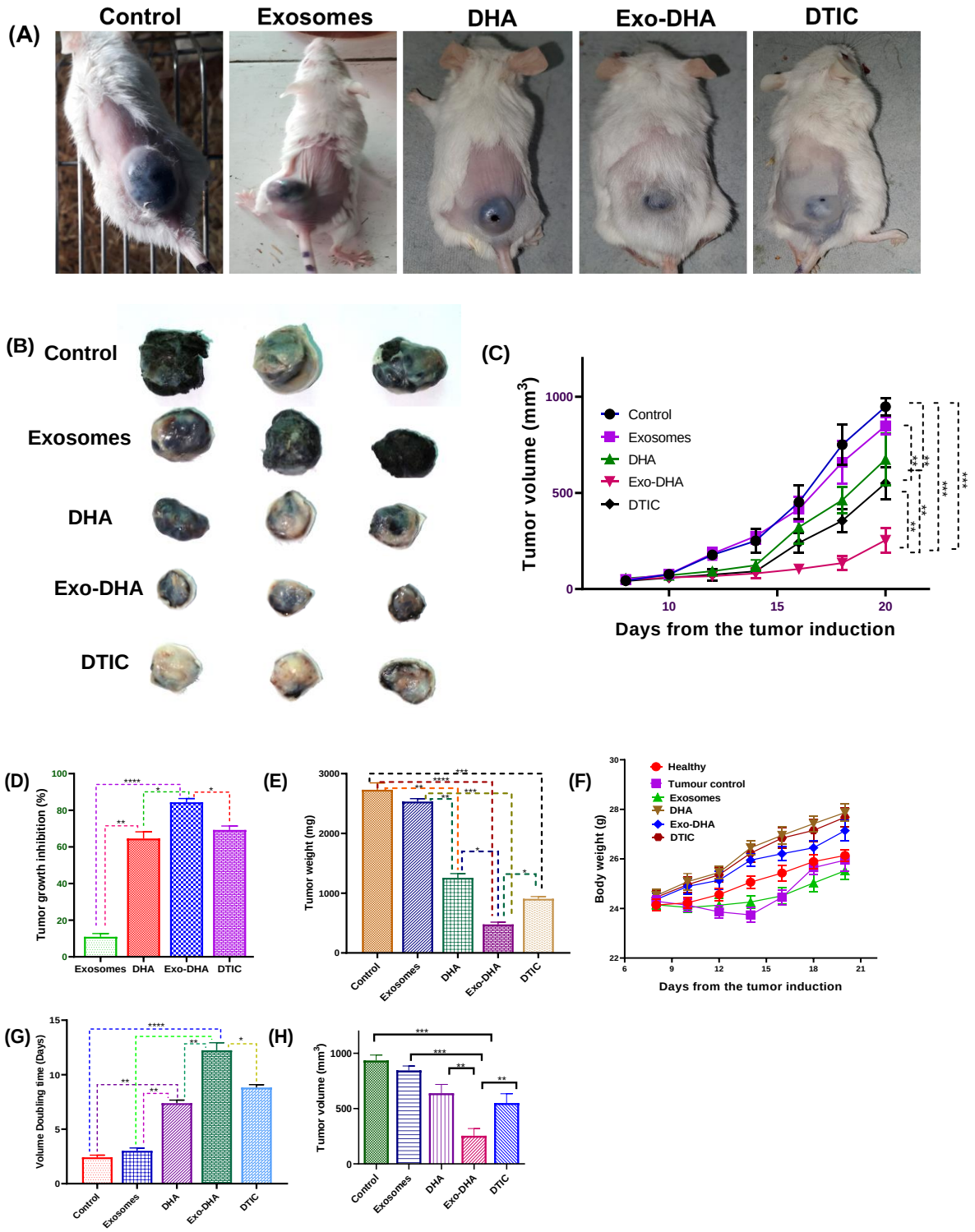

Figure 5.29 *In vivo* DHA and Exo-DHA anti-cancer efficacy against B16F10 melanoma in Swiss albino mice. (A) representative images of animals at endpoint (day 28 of treatment), (B) representative tumors excised after euthanasia, (C) tumor growth kinetics, (D) percent tumor growth inhibition, (E) excised tumor weight, (F) body weight, (G) tumor volume doubling time, and (H) final tumor volume, Statistical analysis was conducted using One-Way ANOVA followed by the Tukey post hoc test for multiple comparisons. The significance levels were denoted as *$p < 0.05$, **$p < 0.01$, and ***$p < 0.001$ to indicate the statistical significance of the results.

Animals were randomly allocated into different treatment groups, with dosing initiated from the 8th day and continued until the 20 day. DHA was administered orally at an equivalent of 50 mg/kg, while DTIC was given at 5 mg/kg via intraperitoneal injection. Various parameters such as final tumor volumes, tumor growth inhibition (TGI), tumor weight, and tumor volume doubling time were evaluated to assess the efficacy of DHA formulations.

The results revealed that the average tumor growth inhibition percentages for animals treated with exosomes, DHA, Exo-DHA, and DTIC were 9.5, 63.5, 83.2, and 71.2%, respectively (Figure 5.29 D). The average final tumor volumes and tumor weights were also significantly reduced in the Exo-DHA group compared to other treatment groups (Figure 5.29 A-C). Additionally, the tumor volume doubling time was notably prolonged in the Exo-DHA-treated animals (Figure 5.29 E-H). Overall, the *in vivo* efficacy study demonstrated that Exo-DHA substantially reduced tumor growth, increased survival rates, and improved the overall anti-cancer efficacy compared to free DHA, highlighting the potential of exosome-based drug delivery systems in enhancing therapeutic outcomes.

5.4.21 Toxicity estimation via biochemical parameters and blood parameters

Biocompatibility is the primary concern for most drug-delivery vehicles and anti-cancer compounds. When the drug or delivery vehicle is found unsafe, it primarily induces systemic or tissue toxicity.

Hence, it is vital to check the compatibility of drugs and vehicles. In this study, we performed total hematology parameters such as RBC, WBC, platelets, hemoglobin, etc., and systemic biochemical parameters such as ALT, AST., etc., after the treatment's completion. The hematology report showed that all the values were within the normal range in all the treated groups (Table 5.13). However, in the biochemical analysis, a significantly ($p < 0.01$) increased level of ALT, AST, ALP, Urea, and creatinine was found in DHA and DTIC-treated groups

(Figure 5.30 A-E). The increased levels of ALT, AST, and ALP could indicate toxicity to the liver. In contrast, increased urea and creatinine levels indicate kidney toxicity parameters.

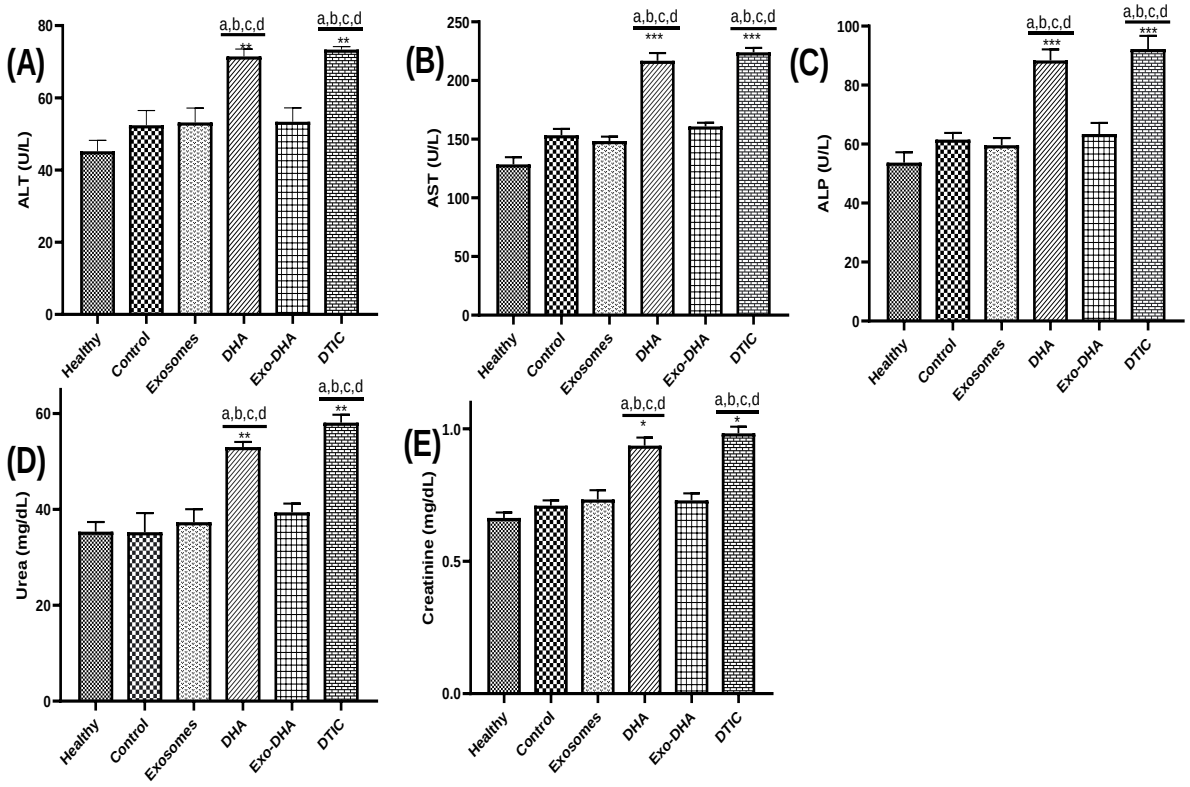

Figure 5.30 Biochemical parameters (A) ALT, (B) AST, (C) ALP, (D) urea, (E) creatinine in plasma after the treatment. a: comparison with healthy, b: comparison with control, c: comparison with exosomes, d: comparison with Exo-DHA. Statistical analysis was performed by One-Way ANOVA followed by the Tukey P test with multiple comparisons and the level of significance *$p < 0.05$, **$p < 0.01$, and ***$p < 0.001$.

Interestingly, no such toxicity was observed in Exo-DHA-treated group animals. This could be due to the accumulation of more drugs at the tumor site in the case of Exo-DHA and more drugs in the liver in the case of DHA and DTIC. On the other hand, the cause of abnormalities due to the DHA and DTIC is still unclear.

Table 5.17 Evaluation of blood parameters after completion of the treatment period

Parameters	Healthy animal	Normal control	Exosomes treated	DHA	Exo-DHA	DTIC
HB (gm/dl)	14.71±0.32	12.52±0.22	12.83±0.81	13.14±0.62	13.71±0.93	13.14±0.42
TLC (/cmm)	9.97±0.41	6.98±0.24	7.46±0.14	7.93±0.14	8.36±0.61	8.14±0.26
WBC (10^3 /L)	9.91±0.27	6.95±0.47	6.46±0.34	7.34±0.73	8.61±0.54	8.22±0.24
Neutrophils (%)	58.77±5.66	41.95±6.21	38.65±8.24	52.45±6.32	57.51±5.55	56.42±6.25
Lymphocytes (%)	67.75±8.62	59.68±9.26	57.54±8.42	63.35±6.95	65.26±7.24	66.46±6.26
Eosinophils (%)	4.12±0.23	2.21±0.08	2.98±0.09	3.65±0.18	3.94±0.99	4.09±0.62
Monocytes (%)	5.23±0.93	3.64±0.45	3.84±0.21	4.62±0.54	4.98±0.86	5.01±0.62
Basophils (%)	0.08±0.01	0.07±0.01	0.07±0.01	0.08±0.01	0.08±0.01	0.08±0.01
RBC (mil/cmm)	9.34±0.12	8.89±0.31	8.62±0.21	9.15±0.25	9.16±0.31	9.16±0.31
PCV (%)	37.32±1.21	38.81±2.38	37.61±3.36	37.48±4.12	37.38±4.21	37.28±3.38
MCV (fl)	43.82±5.62	42.2±6.23	41.6±7.21	43.56±6.84	42.9±7.25	41.9±7.85
MCH (pg)	15.16±1.35	13.92±2.12	13.84±2.23	14.62±3.21	14.74±3.21	14.41±3.51
MCHC (g/dl)	39.92±4.23	35.26±3.56	34.1±4.12	37.4±5.21	37.9±6.12	36.12±4.21
Platelets (lacs/cmm)	7.53±0.51	4.44±0.41	3.77±0.32	5.68±0.39	6.66±0.31	6.68±1.04

Abbreviations:
HB: Haemoglobin; TLC: Total Leucocyte Count; WBC: White blood cells; RBC: Red Blood cells; PCV: Packed cell volume; MCV: Mean corpuscular volume; MCHC: Mean corpuscular hemoglobin concentration; MCH: Mean corpuscular hemoglobin

5.4.22 Histopathology of organs from tumor-bearing mice

To further estimate the signs of toxicity by DHA and DTIC, we have performed the histopathology for vital organs (Heart, Lungs, Liver, Kidney, and spleen) collected from tumor-bearing mice following the treatment and stained with H&E dye. As shown in Figure 5.31, the

hepatocytes and portal vein were found normal in the case of healthy, tumor control, exosomes, and Exo-DHA treated groups. However, the structure of the portal vein was found to be ruptured in the case of the DHA and DTIC-treated groups. This could be due to the damage to sinusoidal endothelial cells causing their death and extrusion into sinusoids with subsequent obstruction. However, such toxicity was not observed in the Exo-DHA-treated groups (Figure 5.31). In addition to hepatotoxicity, no signs of toxicity were observed in the lungs (no pulmonary fibrosis), kidneys (no nephron changes), heart, and spleen. The results indicate that the liver toxicity of DHA was decreased when it was delivered via exosomes.

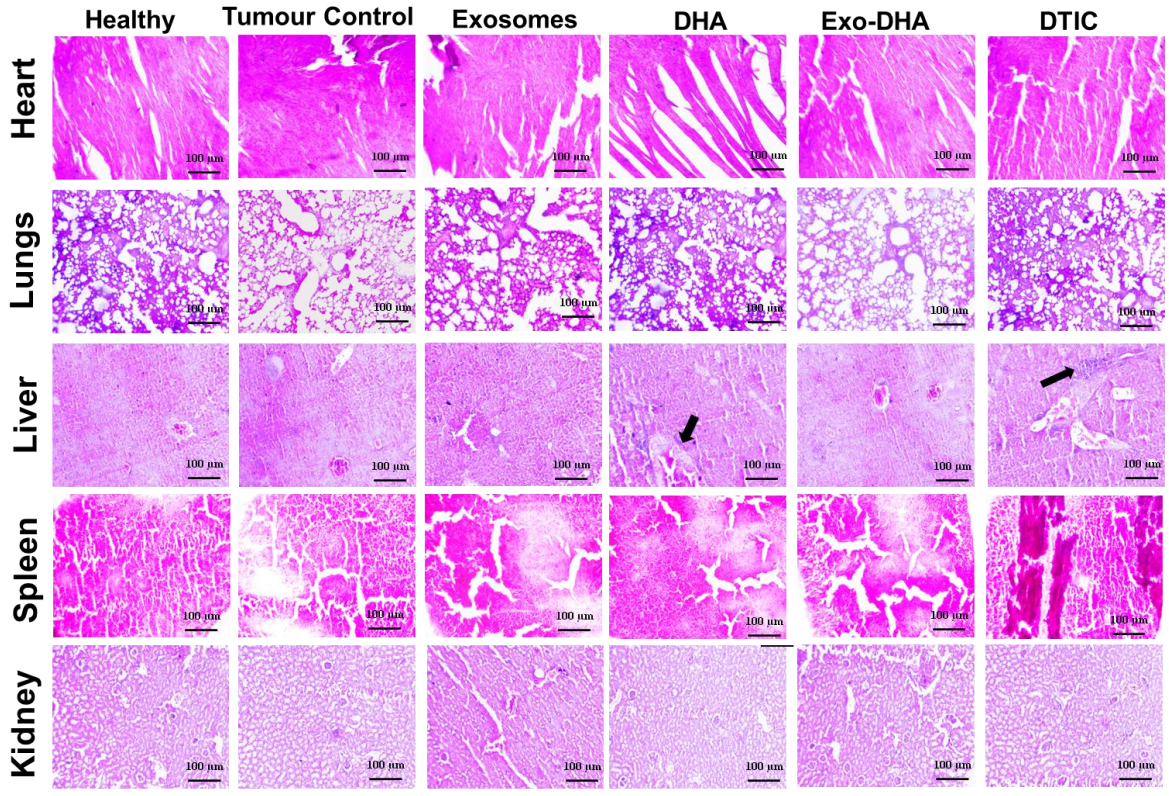

Figure 5.31 Histopathology of H&E stained vital organs isolated from tumor-bearing mice after the treatment. Arrows indicate signs of rupture in portal veins.

5.4.23 *In vivo* tumor migration study

Melanoma's highly metastatic nature poses significant challenges in its treatment and management. It has the propensity to spread to other body parts through systemic circulation, resulting in poor prognosis and making it difficult to treat effectively. Additionally, melanoma

can be resistant to traditional chemotherapy and immunotherapy, further complicating treatment strategies. Therefore, there is a critical need for innovative and targeted approaches to address the challenges posed by metastatic melanoma and improve patient outcomes. A metastasis study was performed to evaluate the improved anti-metastatic properties of Exo-DHA. As shown in Figure 8, the visible migrated cells were found on the lungs, and the number of lung nodules was counted with the naked eye. The number of lung nodules was significantly ($p < 0.05$) low in the Exo-DHA (13±1) treated group compared to the DHA (31±2) treated groups (Figure 5.32 B) and much lower compared to the standard DTIC treatment.

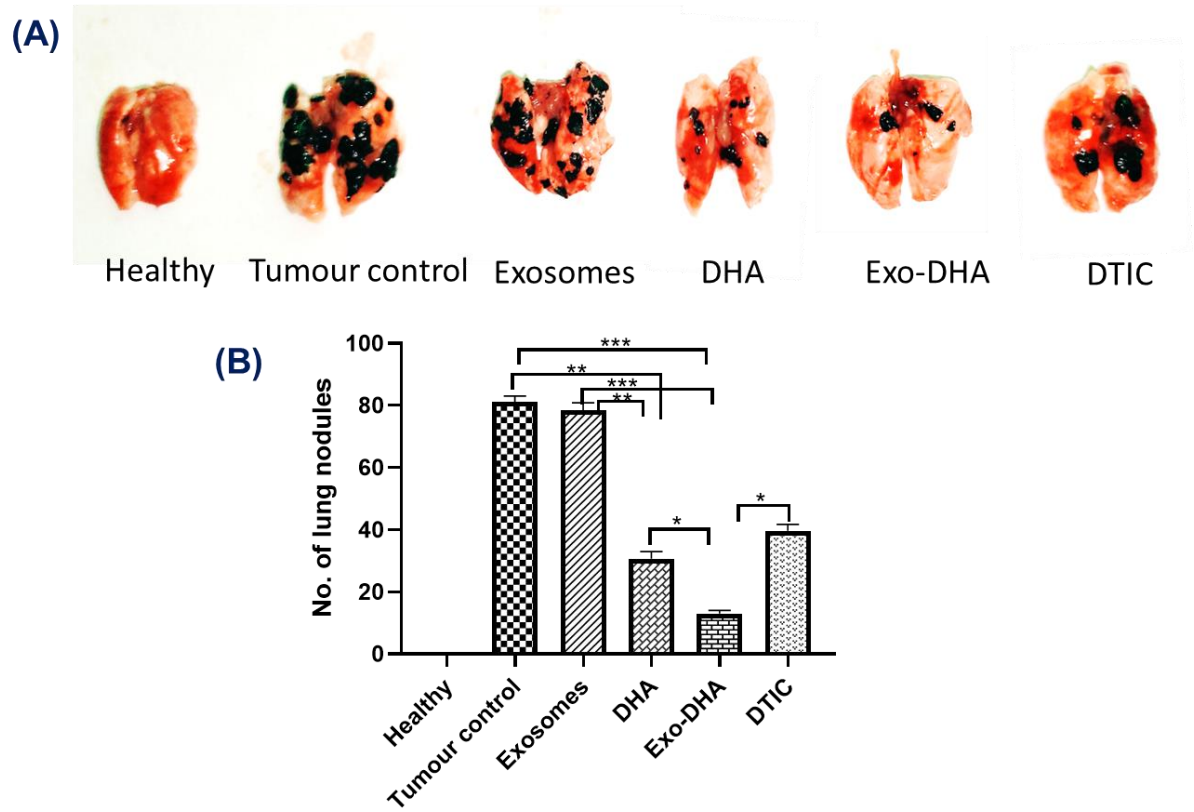

Figure 5.32 An *in vivo* metastasis study was performed in Swiss mice. Exo-DHA significantly decreased the metastatic burden compared to DHA or DTIC treatment. Statistical analysis was performed by One-Way ANOVA followed by the Tukey P test with multiple comparisons and the level of significance *$p < 0.05$, **$p < 0.01$, and ***$p < 0.001$.

The inhibition of metastasis could be due to the inhibition of expression levels of MMP proteins, as confirmed via *in vitro* assay, or the induction of early apoptosis in cancer cells. The inhibition of melanoma metastasis in Swiss mice has been investigated with IFN-α. Further

investigation is required to specify the cellular signaling pathways or mechanisms involved in inhibiting melanoma metastasis by Exo-DHA.

5.5 Conclusion

The current study proposed and investigated the delivery of DHA via bovine milk exosomes to enhance its anti-cancer activity both *in vitro* and *in vivo*. Exosomes were isolated from bovine milk and loaded with DHA using the sonication method, resulting in particles with sizes ranging from approximately 90 to 103 nm, a PDI between 0.119 and 0.123, and a zeta potential ranging from -23 to -28 mV. The improvement in *in vitro* anti-cancer efficacy was confirmed through various assays, including cytotoxicity, apoptosis assay, and western blotting to assess the expression levels of different apoptotic and migration proteins. Furthermore, the study also demonstrated improvements in oral bioavailability, *in vivo* efficacy, toxicity reduction, and metastasis inhibition through different *in vivo* experiments. However, additional *in vivo* studies employing protein expression in *in vivo* samples or RT-PCR are recommended to further validate the mechanism of action of DHA. It would be further beneficial to investigate the efficacy in other animal models to establish the broader applicability and effectiveness of the DHA-loaded exosomes for cancer treatment.

5.6 Summary points

- DHA has shown its treatment potential against melanoma
- Due to the poor water solubility and low oral bioavailability, bovine milk-derived exosomes were used to deliver the DHA.
- DHA was loaded into exosomes via the sonication method, and the BBD approach was employed for the optimization of Exo-DHA formulation.
- DLS results reveal that exosomes were below 150 nm, and HR-SEM and AFM confirmed the spherical shape of exosomes.

- The stability study revealed the prolonged maintenance of physicochemical and pharmaceutical properties without any alterations.
- Exo-DHA formulation showed improved dose-dependent cytotoxicity against B16F10 cells compared to free DHA solution and showed no cytotoxicity towards the noncancerous healthy HEK 293 cell line, reflecting selective cytotoxicity to the cancerous cell.
- Exo-DHA formulation showed improved *in vitro* efficacy compared to free DHA confirmed by various *in vitro* cellular assays.
- The oral bioavailability of DHA significantly improved when loaded into exosomes compared to free DHA.
- The results of the tumor regression study in the syngeneic transplantation melanoma model (in Swiss female mice) revealed improved therapeutic activity of Exo-DHA compared to free DHA.
- Exo-DHA formulations significantly reduced the migration both *in vitro* and *in vivo*.
- The overall result revealed the suitability of exosomes for the delivery of DHA in the treatment of melanoma.